國立台灣大學醫學院分子醫學研究所

博士論文

Graduate Institute of Molecular Medicine

College of Medicine

National Taiwan University

Doctoral Dissertation

探討 EBP50 藉由 Ras-RSK1 訊息傳遞輸送至細胞核

的機制與功能

Mechanistic and Functional Studies of the

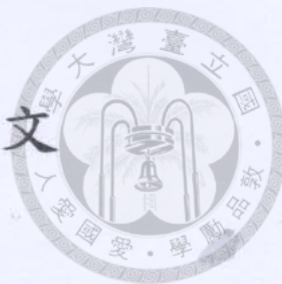Ras-RSK1-regulated Nuclear Transport of EBP50

林慧真

Lim. Hooi Cheng

指導教授: 周祖述教授

Advisor: Jou. Tzuu-Shuh, M.D., Ph.D.

中華民國 104 年 6 月

June 2015

國立臺灣大學博士學位論文
口試委員會審定書

探討 EBP50 藉由 Ras-RSK1 訊息傳遞輸送至細胞核的機制與功能

Mechanistic and Functional Studies of the

Ras-RSK1-regulated Nuclear Transport of EBP50

　　本論文係林慧真君（D97448012）在國立臺灣大學分子醫學研究所完成之博士學位論文，於民國 104 年 6 月 3 日承下列考試委員審查通過及口試及格，特此證明

口試委員：

_____ （簽名）

　　　　　　（指導教授）

_____　_____

_____　_____

_____

系主任、所長 _____ （簽名）

摘要

EBP50（ezrin-radixin-moesin (ERM)-binding phosphoprotein of 50 kDa）在癌症生物學具有爭議性的功能是和此蛋白在各種細胞器的定位息息相關的。位于細胞膜邊緣質體的 EBP50 是抑制癌症的分子，在細胞核內的 EBP50 卻是促進癌症的分子。目前的研究對於 EBP50 進入細胞核的機制並沒有明確的解說。藉由 RNA 干擾 (RNA interference）技術, Ras-ERK 訊息傳遞途徑下游的 RSK1 (p90 ribosomal S6 kinase alpha 1）獲篩選爲可調控 EBP50 輸送至細胞核的關鍵分子。在 EGF (epidermal growth factor) 的調控下，RSK1 與 EBP50 結合並且磷酸化 EBP50 的酥胺酸 156 (T156) 。氨基酸位點突變 (mutagenesis) 實驗進一步確定 T156 在 EBP50 被輸送至細胞核途徑里的關鍵角色。由 RSK1 調控並且會在分裂中的細胞被催化的 EBP50 磷酸化亦會促進 EBP50 和 14-3-3 蛋白的結合，增加細胞分裂和惡性轉化。因此，我們總結由 Ras-RSK1 所催化的 T156 位點磷酸化是 EBP50 被輸送至細胞核的機轉。 我們的研究有助於只針對 EBP50 在細胞核的異常表現而不影響此蛋白的正常生理功能在癌症治療策略的可能性。
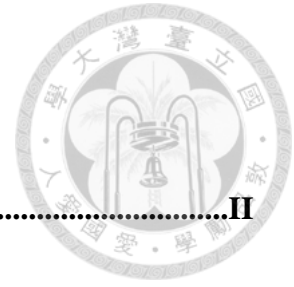
關鍵詞

EBP50; 細胞核定位; 磷酸化; RSK1

ABSTRACT

Differential subcellular localization of Ezrin-radixin-moesin (ERM)-binding phosphoprotein of 50 kDa (EBP50) leads to its controversial role in cancer biology either as a tumor suppressor when it resides at the membrane periphery, or a tumor facilitator at the nucleus. However, the molecular mechanism that regulates nuclear localization of EBP50 remains unclear. A RNA interference screening identified the downstream effector of the Ras-extracellular signal-regulated kinase signaling pathway, p90 ribosomal S6 kinase alpha 1 (RSK1) as the molecule unique for nuclear transport of EBP50. RSK1 binds to EBP50 and phosphorylates it at a conserved threonine residue at position 156 (T156) under regulation of epidermal growth factor. Mutagenesis experiments confirmed the significance of T156 residue in nuclear localization of EBP50. EBP50 phosphorylation by RSK1, which is enhanced in mitotic cells, is also required for recruitment of 14-3-3, cellular proliferation, and oncogenic transformation. Collectively, we discovered the Ras-RSK1-mediated phosphorylation at T156 as the signal underlying nuclear transport of EBP50. Our study sheds light on a possible therapeutic strategy targeting at this aberrant nuclear expression of EBP50 without affecting the normal physiological function of EBP50 at other subcellular localization.

Keywords

EBP50; nuclear localization; phosphorylation; RSK1

TABLE OF CONTENTS

LIST OF ABBREVIATIONS

AGC   Protein kinase A, G and C families

BimEL   Bcl-2 interacting mediator of cell death, extra-long isoform

BPAEC   Bovine pulmonary artery endothelial cells

BRCA1   Breast cancer 1, early onset isoform 1

BSA   Bovine serum albumin

Cdc2   Cyclin-dependent kinase 1 (CDK1)

CRM1   Chromosome region maintenance 1

CTKD   C-terminal kinase domain

DLC1   Deleted in liver cancer 1

DMEM   Dulbecco's modified Eagle's medium

EBP50   Ezrin-radixin-moesin (ERM)-binding phosphoprotein of 50 kDa

EGF   Epidermal growth factor

EGFP   Enhanced green fluorescent protein

EGFR   Epidermal growth factor receptor

ER   Endoplasmic reticulum

ERM   Ezrin-radixin-moesin

ERK   Extracellular signal-regulated kinase

FOXO   Forkhead box O

FRAP   Fluorescence recovery after photobleaching

Gab2   Grb2-associated binder

Gal-3   Galectin-3

GPCR   G protein-coupled receptor

GRK6A   G protein-coupled receptor kinase 6A

GSK3β	Glycogen synthase 3β
GST	Glutathione S-transferase
HEK293	Human embryonic kidney cells
HeLa	Henrietta Lacks cervical adenocarcinoma cells
LMB	Leptomycin B
MAD1	Mitotic arrest deficient-like 1
MDCK	Madin-Darby canine kidney cells
MDM2	Mouse double minute 2 homolog
MUC1	Mucin 1
NES	Nuclear export signal
NHERF1	Na^+-H^+ exchanger regulatory factor 1
NHE3	Na^+-H^+ exchanger isoform 3
NLS	Nuclear localization signal
NPC	Nuclear pore complexes
NTKD	N-terminal kinase domain
PBS	Phosphate-buffered saline
PDK1	3'-phosphoinositide-dependent kinase-1
PDZ	Postsynaptic density 95/disks large/zona occludens
PFA	Paraformaldehyde
PKC	Protein kinase C
PP2A	Protein phosphatase 2A
PTH1R	Parathyroid hormone receptor
RNAi	RNA interference
RSK1	p90 ribosomal S6 kinase alpha 1
R7BP	Regulator of G protein signaling 7 binding protein

shRNA   Short hairpin RNA

SRY   Sex-determining region Y protein

SW480   Human colon adenocarcinoma cells

TBS   Tris-buffered saline

TCF1   T cell factor 1

YAP   Yes-associated protein

LIST OF FIGURES

LIST OF TABLES

INTRODUCTION

1.1   Background

Membrane-bounded subcellular organelles that compartmentalized within the cytoplasm, including the nucleus, endoplasmic reticulum (ER), Golgi complex and mitochondria, are functional specification of eukaryotic cells. Eukaryotic cells organize intracellular molecules in these organelles to maintain specific functions of various molecules. However, cells also consist of multifunctional proteins, which can exert distinct functions depending on their localizations in differential subcellular compartments, where they may possess preferential alterations in its chemical structure, post-translational modifications and/or interaction with other signaling molecules. Therefore, precise targeting of a multifunctional protein to a specific compartment under certain physiological context is crucial to maintain normal cellular functions.

1.2   Protein Subcellular Localization

In eukaryotic cells, protein translation takes place in the cytosol either on free ribosomes or on ER-bound ribosomes, and the newly synthesized proteins needed to be transported to other subcellular compartments for their specific functions. Protein targeting to subcellular organelles occurs through two major mechanisms, co-translational and post-translational translocation, determined by the signal sequence encoded within the protein (Rapoport, 2007; Wickner and Schekman, 2005). Generally, proteins are targeted to the mitochondria or the nucleus by post-translational translocation (Schmidt et al., 2010; Terry et al., 2007), but proteins of secretory pathway and integral membrane proteins are co-translationally transported into the ER (Wickner and Schekman, 2005).

1

1.2.1 Mechanisms of protein mislocalization from/to the nucleus

Post-translationally protein transport across the nuclear envelope is regulated by the nuclear pore complexes (NPCs), which are aqueous channels comprising multiple copies of about 30 distinct proteins grouped as nucleoporins (Raices and D'Angelo, 2012; Wente and Rout, 2010). The NPCs allow passage of small molecules such as ions and metabolites though simple diffusion. However, nuclear transport of larger molecules such as proteins and RNAs are mediated by receptors that recognize specific nuclear localization signal (NLS) or nuclear export signal (NES) encoded within the cargo (Terry et al., 2007).

Genetic alterations involve dysregulated expression of protein trafficking machinery and mutation of targeting signal, are major mechanisms underlying mislocalization of nuclear proteins. The nuclear transport receptor, chromosome region maintenance 1 (CRM1) regulates the nuclear export of many tumor suppressors. Overexpression of CRM1, which causes aberrant cytoplasmic accumulation of p53, breast cancer 1, early onset isoform 1 (BRCA1) or forkhead box O (FOXO), has been proved to be associated with tumorigenesis (Turner et al., 2012). Moreover, missense mutations within two NLSs of the sex-determining region Y protein (SRY) reduce its nuclear localization, and loss of nuclear SRY is associated with Swyer syndrome (Harley et al., 2003).

In addition, protein mislocalization also can happen through indirect mechanisms, including changes in protein-protein interactions and post-translational modification. For example, loss of interaction with p14ARF leads to retention of mouse double minute 2 homolog (MDM2) in the nucleus (Esteller et al., 2001). Covalent lipid modifications, including myristoylation, palmitoylation and farnesylation, are important in the membrane targeting of proteins and their enrichment in microdomains of

2

organelles. The plasma membrane-nuclear shuttling of regulator of G protein signaling 7 binding protein (R7BP) is regulated through palmitoylation, in which palmitoylation of R7BP targets it to the plasma membrane, and depalmitoylation of R7BP translocates the R7BP-R7-$G_\beta 5$ complexes to the nucleus (Drenan et al., 2005).

1.2.2 Protein mislocalization in cancer

Cancer is a multifactorial disease, and the development of cancer involves multiple processes that contributed to continual dysregulated cell proliferation. In addition to genetic alterations, mislocalization of oncoproteins or tumor suppressors is another important mechanism in cancer development and progression. For example, mucin 1 (MUC1) is an oncoprotein that has complex role at different subcellular compartments. Mucins are glycosylated proteins that are either secreted to the extracellular compartments or are bounded with the plasma membrane. Normally, membrane-bound mucin is expressed at the apical borders of glandular epithelial cells. However, localization of mucin was detected at the cytoplasm, mitochondria and the nucleus of carcinoma cells (Kufe et al., 1984). The MUC1 cytoplasmic domain was detected in the nucleus of S2-013 and Panc-1 human pancreatic cancer cells (Wen et al., 2003). Nuclear MUC1 interacts with β-catenin in both the cytoplasm and the nucleus, and co-activates β-catenin-dependent gene transcription to promote tumor growth (Huang et al., 2003; Wen et al., 2003).

In recent years, proteins that are differentially resided in normal cells and tumor cells had become popular drug target. For example, galectin-3 (Gal-3) is translocated from the nucleus to the cytoplasm when cancer cells exposed to the anti-cancer drug cisplatinum; an event that protected cancer cells from drug-induced apoptosis (Takenaka et al., 2004). However, treatment of breast cancer tumor cells with both

cisplatinum and nuclear export inhibitor leptomycin B (LMB) retained Gal-3 in the nucleus and induced cell apoptosis (Takenaka et al., 2004). This study highlights the urge for exploring the mechanism underlying subcellular localization of disease-related proteins.
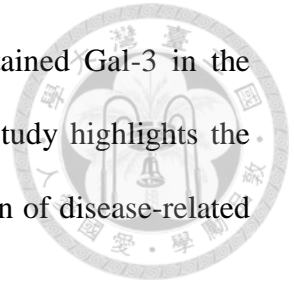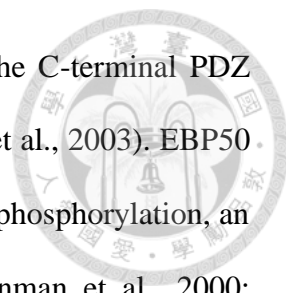
1.3   The PDZ Domain-containing Protein EBP50

Ezrin-radixin-moesin (ERM)-binding phosphoprotein of 50 kDa (EBP50), also known as Na^+-H^+ exchanger regulatory factor 1 (NHERF1), is a scaffold protein that first described as an essential cofactor for cyclic AMP inhibition of Na^+-H^+ exchange in the rabbit renal brush border membrane (Weinman et al., 1995). EBP50 consists of two tandem postsynaptic density 95/disks large/zona occludens (PDZ) domains and a C-terminal ezrin binding site (Reczek et al., 1997). The PDZ domains of EBP50 at the N-terminal region preferably recognize the C-terminal PDZ binding motif (S/T)XL of its interacting partners, while the C-terminal ezrin binding site binds all members of the ERM protein family which organize the cell cortex through interaction with membrane proteins and filamentous actin (Fehon et al., 2010; Reczek and Bretscher, 1998; Shenolikar et al., 2004; Wang et al., 1998).

1.3.1   The scaffolding function of EBP50 at the plasma membrane periphery

The unique protein architecture of EBP50 allows it to organize molecules into functional complexes at the membrane periphery. And thus, early studies of EBP50 were heavily focused on its regulatory roles at the plasma membrane periphery, such as ion transporters activation (Wang et al., 1998; Weinman et al., 2003), receptors recycling (Rochdi and Parent, 2003; Sneddon et al., 2003), and microvillar assembly (Garbett et al., 2010; Hanono et al., 2006). EBP50 was first identified as the interacting

4

partner of Na^+-H^+ exchanger isoform 3 (NHE3), which binds to the C-terminal PDZ binding motif of NHE3 through its second PDZ domain (Weinman et al., 2003). EBP50 facilitates association of NHE3 with ezrin to recruit PKA for NHE3 phosphorylation, an event that leads to downregulation of its transport activity (Weinman et al., 2000; Weinman et al., 2003). For recycling of G protein-coupled receptors (GPCRs), EBP50 has been reported to block thromboxane A (2) beta receptor (TPbeta receptor) internalization (Rochdi and Parent, 2003). In addition, a study in kidney distal tubule cells and rat osteosarcoma cells demonstrated that EBP50 inhibits the antagonist-induced type 1 parathyroid hormone receptor (PTH1R) endocytosis (Sneddon et al., 2003). The plasma membrane of differentiated epithelial cells polarized into compositionally distinct apical and basolateral membrane. The apical surface of epithalial cells usually featured with microvilli, which consist of a core of bundled actin filaments linked to the plasma membrane partly through ezrin (Fehon et al., 2010). A previous study reported that depletion of EBP50 in human chriocarcinoma JEG-3 cell causes loss of microvilli as observed by actin and ezrin staining (Hanono et al., 2006). Later study demonstrated that EBP50 phosphorylations by Cdc2 and PKC are required for microvillar assembly (Garbett et al., 2010).

1.3.2 Subcellular localization of EBP50 modulates its cellular functions

EBP50 is mainly expressed at the apical surface of luminal organs (Fouassier et al., 2001; Lecce et al., 2011; Reczek et al., 1997). Under physiological conditions, EBP50 is localized at the apical brush border membrane of intestinal epithelial cells, in which it interacts with β-catenin to maintain localization of β-catenin at the cell-cell junction to maintain the integrity of epithelial tissues through inhibition of cell motility and suppression of anchorage independent growth (Kreimann et al., 2007). A study in

three-dimensional model of developing human intestinal glands also reported that depletion of EBP50 causes membrane displacement of phosphatase and tensin homolog (PTEN) and nuclear translocation of β-catenin, events contributing to polarity loss and increased proliferation (Georgescu et al., 2014). Furthermore, EBP50 interacts with pleckstrin-homology domain leucine-rich repeat protein phosphatases (PHLPP) and scaffolds it with PTEN to form a tumor suppressor complex, which inhibits the oncogenic phosphatidylinositol-3-OH kinase (PI3K)-Akt signaling pathway (Molina et al., 2012). These findings had once leaded to the conclusion that EBP50 is a tumor suppressor.

Nevertheless, EBP50 was later found localized at the nucleus in cultured cell lines such as cholangiocarcinoma line Mz-Ch-A1 and colon adenocarcinoma line SW480, as well as specimens of hepatocellular, colorectal and breast cancer (Fouassier et al., 2009; Lin et al., 2012; Malfettone et al., 2012; Mangia et al., 2012; Paradiso et al., 2013; Shibata et al., 2003). In Mz-Ch-A1 cells, stimulation with estrogen enhances nuclear localization of EBP50 (Fouassier et al., 2009). Moreover, localization of EBP50 to the nucleus was also reported in human cholangiopathies and bile duct-ligated rats. (Fouassier et al., 2009). However, the molecule and signaling pathway specific for aberrant nuclear localization of EBP50 are undefined. Study on colorectal cancer reported a re-distribution of EBP50 from apical membrane to cytoplasmic and nuclear localization, and, the nuclear localization of EBP50 is strongly associated with invasive phenotype of colorectal cancer (Lin et al., 2012; Malfettone et al., 2012; Mangia et al., 2012). On the other hand, loss of nuclear EBP50 expression in breast cancer is associated with reduced survival, in which nuclear localization of EBP50 is correlated with small tumor size and positive estrogen receptor expression (Paradiso et al., 2013).

1.4 The RSK Family of Protein Kinases

The p90 ribosomal S6 kinases (RSKs) are a family of AGC kinases consists of four isoforms, named as RSK1-4, which have two kinase domains, an extracellular signal-regulated kinase (ERK) docking motif (also known as the D domain), and a C-terminal PDZ binding motif (Anjum and Blenis, 2008; Lara et al., 2013). The C-terminal kinase domain (CTKD) of RSK is responsible for its activation through autophosphorylation, whereas the N-terminal kinase domain (NTKD) is essential for the phosphorylation of its substrates (Chen et al., 1992; Jensen et al., 1999). Upon stimulation of cells with growth factors, ERK is phosphorylated downstream of the Ras cascade. The activated ERK initiates activation of the CTKD of RSK, via docking at the D domain and phosphorylating RSK1 at threonine573 (T573) residue (Roux et al., 2003; Zhao et al., 1996). Then, the activated CTKD autophosphorylates RSK at serine380 (S380), and creating a docking site for 3'-phosphoinositide-dependent kinase-1 (PDK1); PDK1 phosphorylates the NTKD at S221, resulting in complete RSK activation (Anjum and Blenis, 2008; Jensen et al., 1999).

1.4.1 Subcellular localization of RSKs

In resting cells, inactive RSKs are mainly localized at the cytoplasm (Romeo et al., 2012). Mitogen-stimulated and ERK-dependent activation of RSKs lead to their nuclear translocation. Before translocation to the nucleus, epidermal growth factor (EGF)-stimulated RSK1 transiently associates with the plasma membrane, an event which regulated by the N-terminal myristoylation, but independent of ERK activity (Richards et al., 2001). Only a fraction of active RSKs enter the nucleus, and thus active RSKs have both cytoplasmic and nuclear substrates (Lara et al., 2013; Romeo et al., 2012).

1.4.2 Role of RSKs in cancer biology

RSK genes are not frequently amplified or mutated in cancer lesions; however, RSK proteins, as the immediate downstream effector of the Ras-ERK signaling pathway, are important players in cancer development and progression, through regulation of cell proliferation, apoptosis, and cell migration (Anjum and Blenis, 2008; Lara et al., 2013; Liu et al., 2011; Romeo and Roux, 2011). Mitogen-activated RSKs was shown to phosphorylate several transcription factors and responsible for transcriptional regulation of genes involved in cell proliferation. Skin papilloma development was delayed in *Rsk2*-deficient mice, and this was shown related to RSK2-mediated phosphorylation of c-Fos which promotes cell cycle progression (Bakiri et al., 2011). Similarly, RSK1 phosphorylate mitotic arrest deficient-like 1 (MAD1), a tumor suppressor member of the MYC/MAD/MAX family; RSK1-mediated phosphorylation causes proteasomal degradation of MAD1, thereby promoting MYC-dependent cell proliferation (Zhu et al., 2008). RSKs also exhibit their cancer-promoting role through negative regulation of apoptosis. RSK1/2 phosphorylates the pro-apoptotic tumor suppressor BimEL (Bcl-2 interacting mediator of cell death, extra-long isoform) to facilitate its binding and degradation through the F box protein βTrCP (Dehan et al., 2009). A study in Madin-Darby canine kidney (MDCK) cells using knockdown and pharmacological inhibitor-based approaches reported that RSK is essential to induce mesenchymal motility and invasion (Doehn et al., 2009). In contrast, RSK-mediated phosphorylation of Gab2 was shown to inhibit migration of mammary epithelial MCF-10A cells (Zhang et al., 2013).

1.5   Objectives

Multifunctional cellular proteins can exhibit opposing functions depending on its subcellular localization. Understanding the protein trafficking mechanisms is, thus, an important basis for physiological defects that eventually lead to disease development. EBP50, through its two PDZ domains, interacts with a wide range of signaling proteins that reside at differential subcellular compartments, ranging from transporters and receptors at the plasma membrane to transcription factors at the nucleus. However, EBP50 lacks a clear NLS, and the molecular mechanism for its nuclear localization remains unclear. This study aims to investigate the protein and signaling pathway specific for nuclear localization of EBP50, which may provide new insight into therapeutic strategy towards oncogenic nuclear EBP50 without affecting its functions at other subcellular compartments.
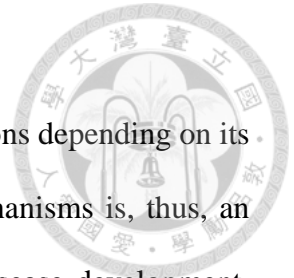
MATERIALS AND METHODS

2.1 Materials

2.1.1 Plasmids

The EBP50 cDNA was cloned into pEGFP-C1 vector (BD Biosciences, Lexington, KY, USA) at *Xho*I and *BamH*I sites to generate a plasmid expressing EGFP-tagged EBP50 (pEGFP-EBP50). Mutations in the phosphorylation motif of EBP50 were introduced using mutagenic primers and PCR of pEGFP-EBP50 plasmid (Table 1). Plasmids expressing glutathione S transferase (GST)-fused full length EBP50 and its individual PDZ domains were constructed by in-frame cloning of the corresponding cDNA fragments into pGEX vector (Clontech, Mountain View, CA, USA). All the above constructs were sequence verified. Plasmids expressing HA-tagged wild type RSK1, myristoylated constitutively active (Myr-RSK1) and kinase dead (RSK1-KD) mutants were kind gift from Philippe Roux (University of Montreal, Montreal, Canada). Plasmid expressing HA-tagged constitutively active Ras (RasV12) was kind gift from Hong-Chen Chen (National Chung Hsing University, Taichung, Taiwan). Plasmids expressing GST-fused 14-3-3 proteins were kind gift from Monilola A. Olayioye (University of Stuttgart, Stuttgart, Germany).

2.1.2 Chemicals

The following chemicals were used: protease inhibitor cocktail (Sigma-Aldrich, St. Louis, MO, USA), phosphatase inhibitor cocktail (Roche Diagnostic, Basel, Switzerland), purified human EGF (Invitrogen, Carlsbad, CA, USA), Calyculin A (Cell Signaling Technology), purified PP1 and PP2A (Millipore), thymidine (Sigma-Aldrich), nocodazole (Sigma-Aldrich), and Leptomycin-B (Sigma-Aldrich).

2.1.3 Antibodies

The following antibodies were used: mouse anti-EBP50 antibody (BD Biosciences, San Jose, CA, USA), rabbit anti-EBP50 antibody (Abcam, Cambridge, MA, USA), rabbit anti-RSK1 antibody and rabbit anti-phospho RXRXXS/T antibody (Cell Signaling Technology, Beverly, MA, USA), rabbit anti-phospho RSK1 (S380) antibody (Millipore, Billerica, MA, USA), mouse anti-HA antibody, mouse anti-α-tubulin antibody (gift from Sheng-Chung Lee, National Taiwan University, Taipei, Taiwan), mouse anti-Ezrin antibody (Lab Vision, Fremont, CA, USA), rabbit anti-GFP antibody and mouse anti-GFP antibody (GeneTex, Hsinchu, Taiwan), mouse anti-Myc antibody (9E10 hybridoma clone from ATCC, Manassas, VA, USA). Anti-phospho-EBP50 (T156) antibody was generated by immunizing rabbits with a synthetic phosphopeptide (LRPRLS(pT)MKKGPSC) and was purified using affinity chromatography.

2.2 Methods

2.2.1 Cell culture and transfection

HeLa, HEK293, SW480, and MDCK cells were cultured in Dulbecco's modified Eagle's medium (DMEM) supplemented with 10% fetal bovine serum and penicillin/streptomycin/ampicillin at 37°C in a humidified incubator containing 5% CO_2. Plasmids were delivered to the cells using Lipofectamine 2000 (Invitrogen) according to the manufacturer's instructions. HeLa cells stably expressing EGFP-EBP50 (HeLa-EGFP-EBP50 cells) were selected with 500 μg/ml of G418 (Invitrogen). To generate HeLa cells that stably expressed the phospho-mutants of EBP50 at T156, cells were first infected with EBP50 shRNA lentivirus to knockdown endogenous EBP50 (Table 2). After the knockdown efficiency of EBP50 was confirmed, these

11

stable cells were transfected with shRNA resistant phospho-mutants and wild type EBP50 expressing plasmids (Figure 8A) following G418 selection. The protein expression level of these cells were analysed by Western blotting (Figure 8B).
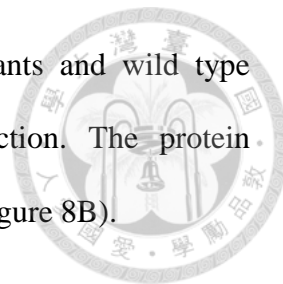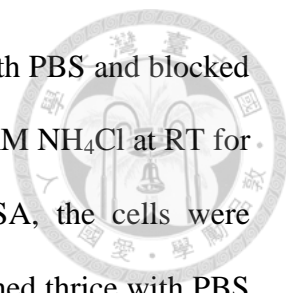
2.2.2 RNAi screening

A shRNA library for human genes of enzymes involved in protein post-translational modifications, including phosphorylation, ubiquitination and palmitoylation were obtained from the Academia Sinica RNAi Core Facility, Taipei, Taiwan (Appendix I). In this library, individual genes is targeted by 3 to 5 independent short hairpin sequences carried in lentiviral vectors that arrayed in 96-well plates. HeLa-EGFP-EBP50 cells were plated a day before infection with shRNA lentiviruses using Biomek FX-P Laboratory Automation Workstation (Beckman Coulter, Brea, CA, USA). At 24 h after lentiviral infection, the transduced cells were selected with puromycin for 72 h, and then fixed with 3.7% (w/v) paraformaldehyde (PFA) before being imaged using Cellomics Arrayscan VTI High Content System (Thermo Scientific, Waltham, MA, USA). The Molecular Translocation Bioapplication of the equipped Cellomics software (Thermo Scientific) was used for image analysis. The mean difference in average EGFP fluorescence intensity between the nucleus and the cytoplasm (EGFP N-C) of triplicate experiment was used to quantify the nuclear translocation of EBP50.

2.2.3 Immunofluorescence staining and microscopy

HeLa cells plated onto coverslips the night before the experiments were washed twice with phosphate-buffered saline (PBS) and then fixed with 3.7% (w/v) PFA. Permeabilization was carried out by incubation with CSK buffer (50 mM NaCl, 300 mM sucrose, 10 mM Pipes at pH 6.8, 3 mM $MgCl_2$, and 0.5% (v/v) Triton-X100) at

room temperature (RT) for 10 min. Cells were then washed twice with PBS and blocked with PBS containing 1% (w/v) BSA, 10% (v/v) goat serum and 50 mM NH_4Cl at RT for 1 h. After washing briefly with PBS containing 0.2% (w/v) BSA, the cells were incubated with primary antibody at RT for 1 h. Cells were then washed thrice with PBS containing 0.2% (w/v) BSA, and incubated with secondary antibody at RT for 1 h. After washing thrice with PBS containing 0.2% (w/v) BSA, cells were mounted in Vectashield medium (Vector Laboratories, Burlingame, CA). Images were acquired with Zeiss LSM780 confocal microscope (Carl Zeiss Jena GmbH, Jena, Germany) using a 40x or 63x oil immersion objective.

2.2.4 Immunoprecipitation and Western blotting

Cells were lysed in CSK buffer containing protease and phosphatase inhibitor cocktails plus 1 mM DTT at 4°C for 1 h. Clarified cell lysates containing equal amounts of protein were incubated with protein A bead-bound anti-GFP antibody at 4°C for 4 h. Beads were then washed for three times with CSK buffer and boiled in 2x SDS sample buffer. The immunoprecipitated materials were separated by SDS-PAGE followed by Western blotting analysis using appropriate antibodies. For Western blotting, proteins were blotted onto nitrocellulose membrane and blocking was performed in 5% milk/PBST (PBS containing 0.05% Tween-20). The membranes were incubated with primary antibody overnight at 4°C followed by washes thrice with PBST and vigorous shaking. Then, the membranes were incubated with horseradish peroxidase-conjugated secondary antibodies (GE Healthcare, Buckinghamshire, UK) at RT for 1 h, and visualization was performed using enhanced chemiluminescence reagents (Perkin Elmer, Waltham, MA, USA) and exposure to X-ray film (GE Healthcare). When using

phosphospecific antibodies as the primary antibody to detect phosphorylated antigens, the buffer system was replaced with Tris-buffered saline (TBS).

2.2.5 GST pull-down and *in vitro* competition assays

The GST-fused full length EBP50 and its individual PDZ domains, or GST-fused 14-3-3 proteins were produced in *Escherichia coli* BL21 strain and conventionally purified on glutathione-Sepharose 4B beads (GE Healthcare) in PBS containing 4 mM 2-Mercaptoethanol (Sigma-Aldrich) and protease inhibitor cocktail. For interaction between EBP50 and RSK1, HeLa cells that transfected with plasmids expressing wild type RSK1 or the PDZ binding motif deletion mutant (RSK1deSTTL) were lysed in CSK buffer. GST, GST-EBP50, GST-PDZ1 or GST-PDZ2 captured on Sepharose 4B beads was mixed with the respective cell lysate and incubated overnight at 4°C. The beads were then washed with CSK buffer three times with intermittent sedimentation by centrifugation. Pulled down proteins collected by boiling in SDS sample buffer were resolved by SDS-PAGE and analysed by Western blotting. For peptide competition assay, cell lysate was incubated with GST-14-3-3β in the absence or presence of synthetic phosphopetide targeted T156 of EBP50 (Figure 6B), followed by Western blotting analysis for interaction between EBP50 and 14-3-3β.

2.2.6 *In vitro* kinase assay

HA-tagged wild type or kinase dead mutant RSK1 were immunoprecipitated from transfected HEK293 cells that lysed in CSK buffer. Immunoprecipitates were then washed twice in CSK buffer and twice in kinase buffer (25 mM Tris at pH 7.5, 2 mM DTT, 10 mM $MgCl_2$, and phosphatase inhibitor cocktail). Kinase assays were carried out with purified GST-EBP50 at 37°C for 30 min in the kinase buffer supplemented

with 0.5 mM ATP. The samples were subjected to SDS-PAGE and Western blotting analysis.

2.2.7 *In vitro* dephosphorylation assay

0.1 μg of synthetic phosphopeptide that flanks the RXRXXpS/T motif of EBP50 was incubated with 0.1 unit of purified PP1 in PP1 reaction buffer (50 mM Tris-HCl at pH 7.0, 0.1 mM EDTA, 5 mM DTT, 0.01% v/v Triton X-100, and 1 mM $MnCl_2$), or purified PP2A in PP2A reaction buffer (20 mM HEPES at pH 7.0, 1 mM DTT, 1 mM $MgCl_2$, and 100 mg/ml BSA) at 30°C for 1 h in the absence or presence of 100 nM Calyculin A. The phosphorylation of the peptide was analysed by immune-dot blot assay using anti-phospho EBP50 (T156) antibody.

2.2.8 FRAP experiment

Cells were seeded on 35 mm glass-bottom culture dishes (ibidi GmbH, Planegg, Germany). For nuclear import analysis, nuclear export of serum-starved cells was blocked with 10 ng/ml of Leptomycin B 1 h before FRAP experiments. FRAP assays were carried out on Zeiss LSM780 confocal microscope with an environmental chamber maintained at 37°C and 5% CO2 throughout the experiment. Bleaching was performed at 100% laser intensity on the entire nuclear fluorescence using 30 cycles. The recovery of fluorescence was recorded by taking images at 10 s interval using a 63x oil immersion objective. Mean nuclear fluorescence intensities were measured using the region of interest (ROI) function of ZEN 2011 software (Carl Zeiss Jena GmbH) after background subtraction. Nuclear fluorescence recovery was calculated by setting the mean nuclear fluorescence of bleached image as 1. Analysis was performed on 14 cells for each stable clone.

2.2.9 Cell proliferation assay

Cell proliferation was assayed using commercially available MTS tetrazolium reagent, the CellTiter 96® Aqueous One Solution (Promega, Madison, WI, USA). Briefly, 1×10^3 cells were seeded in 96-well plates and incubated for the indicated periods before 20 µl MTS reagent were added. The absorbance at 490 nm was recorded after 4 h incubation with MTS reagent. The experiment was carried out in triplicates.

2.2.10 Soft agar assay

1.5×10^3 cells were mixed with DMEM containing 0.4% agar (Lonza, Basel, Switzerland) and 10% FBS. The cells suspension was then poured onto a solidified 0.6% agar that prepared in 24-well plates. Cells were incubated for 12 days before stained with 0.05% cresyl violet (Sigma-Aldrich) for colonies counting.

2.2.11 *In vivo* tumorigenesis study

Cells were trypsinized, washed with PBS and suspended in DMEM/Matrigel basement membrane matrix (BD Biosciences) at a ratio of 1:1 (v/v). 5×10^6 cells were then injected subcutaneously at the dorsal sites of 8 weeks old NOD/SCID mice. The animals were monitored for tumor growth, and tumor sizes were measured 4 weeks after injection. All mice were treated according to guidelines for experimental animal use specified by the National Taiwan University College of Medicine.

2.2.12 Data analysis
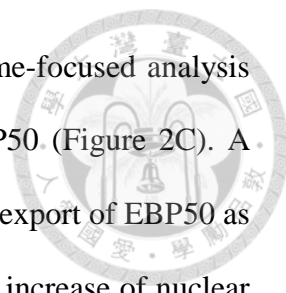
All data are presented as mean $\pm$ SEM. Differences in the mean values between 2 groups were determined by Student's *t*-test, and *p* value less than 0.05 is considered statistically significant

RESULTS

3.1 Ras-RSK1 Signaling Promotes Nuclear Localization of EBP50

The literature reported interacting partners of EBP50 was reviewed and categorized based on their subcellular localization (Shenolikar et al., 2004) (Figure 1). In addition to membrane and cytoplasmic proteins, EBP50 was demonstrated to interact physically with proteins that shuttle between cytoplasm and nucleus, including G protein-coupled receptor kinase 6A (Hall et al., 1999), epidermal growth factor receptor (Claperon et al., 2012), and Yes-associated protein (Mohler et al., 1999), as well as the nucleus-localized Wnt responsive transcription factor TCF1 (Lin et al., 2012). This finding is in accordance with the recent understanding about EBP50, a scaffold protein that not only organizes molecular complexes at the membrane periphery, but is also found localized at the nucleus of cultured epithelial cells and carcinoma specimens (Fouassier et al., 2009; Lin et al., 2012; Shibata et al., 2003). To discover the molecular and signaling pathway governing the nucleocytoplasmic transport of EBP50, a HeLa cell clone that stably expressed enhanced green fluorescent protein (EGFP)-tagged EBP50 (HeLa-EGFP-EBP50) was generated. This cell line was subjected to an arrayed RNA interference (RNAi) screening (Figure 2A) based on the premise that post-translational modification of EBP50, a highly phosphorylated protein, would likely affect its subcellular localization. A total of 1356 genes encoding enzymes that are involved in protein phosphorylation, ubiquitination and palmitoylation were included in this screening (Figure 2B). The changes in the distribution of EGFP signals between nucleus and cytoplasm of shRNA lentiviral-infected HeLa-EGFP-EBP50 cells were automatically quantified on a platform as described in the methodology section 2.2.2 and scored for potential modulators in the nuclear trafficking of EBP50 (Figure 2C and

Appendix I). As expected, most of the genes included in this kinome-focused analysis had insignificant effect on the nucleocytoplasmic transport of EBP50 (Figure 2C). A total of 11 genes were identified as the potential regulator in nuclear export of EBP50 as knockdown of the candidate gene each resulted in a more than 50% increase of nuclear EBP50 (Figure 3 and Appendix I). On the other hand, depletion of RSK1 by two independent lentiviral clones significantly reduced nuclear accumulation of EBP50 (Figure 4A and Appendix I). RSK1 is the downstream effector of the Ras-ERK signaling pathway which phosphorylates and activates many nuclear transcriptional factors (Bonni et al., 1999; Chen et al., 1993; Wu and Janknecht, 2002). Accordingly, overexpression of the constitutively active oncogenic Ras (RasV12) promoted nuclear localization of EBP50 (Figure 4B). Furthermore, increased nuclear localization of EBP50 was also observed in cells that overexpressed constitutive active mutant of RSK1 (Figure 4C). Taken together, these results demonstrate that Ras-RSK1 signaling promotes nuclear localization of EBP50.
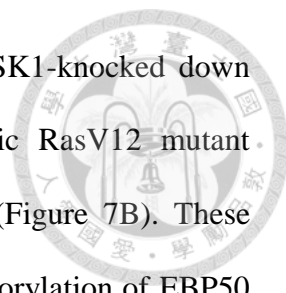
3.2 RSK1 Binds to EBP50 through a PDZ Domain Interaction

EBP50 preferably recognizes the C-terminal PDZ binding motif (S/T)XL, through its two PDZ domains, commonly found in a broad range of its interacting partners which is also noticed in RSKs (Figure 5A). To investigate the potential interaction between EBP50 and RSK1, GST-fused full length EBP50 and its truncated mutants were employed to interact with exogenous RSK1 that was expressed transiently in HEK293 cells in a pull-down assay. Indeed, the result indicated that RSK1 binds to the first PDZ domain of EBP50 through its C-terminal PDZ binding motif as deletion of the terminal 4 amino acids from RSK1 abolished this interaction (Figure 5B). The physical association of RSK1 with EBP50 was further confirmed by reciprocal co-

immunoprecipitation studies in HeLa cells (Figures 5C and 5D). Interestingly, the association of RSK1 with EBP50 was stimulated by EGF in HeLa cells, which quickly fell to the resting status within a time span of less than 60 min (Figure 5E). Collectively, we identified RSK1 as a novel binding partner of EBP50 that binds to EBP50 at its first PDZ domain. Moreover, this interaction is dynamic and subjective to a tight regulation.

3.3   RSK1 Phosphorylates EBP50 at the RXRXXpS/T Motif
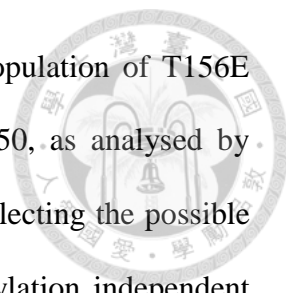
Ras-ERK-dependent activation of RSK induces phosphorylation of both cytoplasmic and nuclear proteins possessing the RXRXXpS/T consensus phosphorylation motif (Leighton et al., 1995). This AGC kinases consensus phosphorylation motif is also present in human, rat and mouse sequences of EBP50 (Figure 6A). Conservation of the RXRXXpS/T motif among mammalian EBP50 signifies the potential of EBP50 as a candidate substrate of AGC kinases such as RSK1. A previous proteomic approach on human T lymphocyte Jurkat cells using an antibody recognizing phosphorylation at the RXRXXpS/T motif had identified EBP50 as a potential substrate phosphorylated at this motif (http://www.phosphosite.org/proteinAction.do?id=4000&showAllSites=true). To definitively examine if EBP50 could serve as a substrate of RSK1, phospho-T156 antibody that recognizes phosphorylation of human EBP50 at the RXRXXpS/T motif was generated by immunizing rabbits using synthetic phosphopeptide (Figure 6B). Dot blot analysis demonstrated that this antibody recognizes the antigenic phosphopeptide, but not the control peptide (Figure 6C). Phosphorylation of EBP50 at T156 was then analysed in HeLa cells that re-stimulated with serum after 48 h of starvation. The result shows that, following serum stimulation for 7 h, EBP50 was phosphorylated at T156 up to the level as when cells were grown in optimal media (Figure 7A). By contrast, serum-

19

stimulated phosphorylation of EBP50 was significantly less in RSK1-knocked down cells (Figure 7A). Furthermore, overexpression of the oncogenic RasV12 mutant enhanced phosphorylation of EBP50 at T156 in HEK 293 cells (Figure 7B). These results indicate the essential role of Ras-RSK1 signaling for phosphorylation of EBP50 at T156. To demonstrate specifically that RSK1 indeed is the kinase directly responsible for phosphorylation of EBP50 at the RXRXXpS/T motif, recombinant RSK1 was purified from HEK293 for an *in vitro* kinase assay. This assay showed that EGF-activated HA-tagged wild type RSK1, but not the kinase dead mutant, could phosphorylate recombinant EBP50 protein at the RXRXXpS/T motif (Figure 7C). RSK1-mediated site-specific phosphorylation of EBP50 at T156 was further confirmed by an independent *in vitro* kinase assay, using synthetic peptide as substrate (Figure 7D). Furthermore, protein phosphatase 2A (PP2A) was discovered as the phosphatase that regulates phosphorylation of EBP50 at T156 (Figure 7E). In summary, RSK1 phosphorylates EBP50 at T156 that lies within the conserved RXRXXpS/T motif, and this phosphorylation event could be regulated by PP2A.

3.4 EBP50 T156 Phosphorylation is related to Increased Nuclear Localization
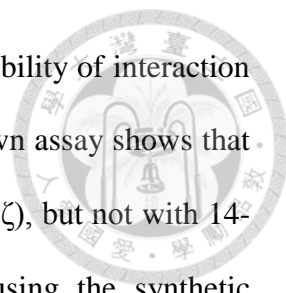
To test the hypothesis that RSK1 regulates nuclear localization of EBP50 through phosphorylation, one of the best understood post-translational modifications underlying nuclear transport, phospho-mutant constructs of EBP50 at T156 was generated (Figure 8A) and then stably expressed in endogenous EBP50-knocked down HeLa cells. Western blotting analysis indicated the expression level of endogenous EBP50 was efficiently replaced by the phospho-mimetic (T156E) or phospho-resistant (T156A) mutants which were then used in subsequent assays (Figure 8B). For cells grown in optimal media containing 10% (v/v) serum, the T156A mutant demonstrated a

marked decrease in nuclear accumulation; while slightly higher population of T156E mutant was observed at the nucleus compared to wild type EBP50, as analysed by quantitative immunofluorescence staining (Figure 9A), probably reflecting the possible involvement of other mechanisms which act on a T156 phosphorylation independent way to govern EBP50 trafficking. The function of T156 on the dynamic of EBP50 subcellular distribution was also investigated *in vivo* using fluorescence recovery after photobleaching (FRAP) approach. To specifically study the nuclear import of EBP50, serum-starved cells at resting state were treated with LMB, an inhibitor of proteins nuclear export (Wolff et al., 1997), an hour prior to experiments. Inhibition of proteins nuclear export using LMB in HeLa cells leads to accumulation of EBP50 in the nucleus (Figure 9B). An increased nuclear EBP50 was also observed in EGF-treated cells, the growth factor that initiates activation of RSK1 (Figure 9B). For FRAP experiments carried on serum-starved resting cells not favoured for phosphorylation at T156, the nuclear import rate of T156A mutant was similar to that of wild type protein. However, the T156E mutant was recovered inside the photobleached-nuclear area much faster (Figure 9C).

3.5   Phosphorylation of EBP50 at T156 Promotes its Binding to 14-3-3β

14-3-3 proteins are a family of dimeric molecules that associate with other proteins in a serine/threonine (S/T) phosphorylation-dependent manner (Yaffe et al., 1997). The phosphorylated S/T residue of many 14-3-3 interacting proteins lies within the consensus phosphorylation motif of RSK (Galan et al., 2014; Yang et al., 2006). Thereby, the 7 isoforms of 14-3-3 proteins have high tendency to bind substrates of RSK, among the reported interactions including son of sevenless homologue 1 (Saha et al., 2012), apoptotic protease activating factor 1 (Kim et al., 2012), and programmed

cell death protein 4 (Galan et al., 2014). Given this reason, the possibility of interaction between 14-3-3 proteins and EBP50 was investigated. GST pull-down assay shows that EBP50 associates with 5 isoforms of 14-3-3 proteins (β, η, ε, γ, and ζ), but not with 14-3-3σ and 14-3-3τ (Figure 10A). A competitive binding assay using the synthetic phosphopeptide T156P, which targeted at the T156 phosphorylation site of EBP50 by RSK1 (Figure 6B), was applied to explore if this phosphorylation is required for recruitment of 14-3-3 proteins. The result shows that perturbation from the competitive peptide reduced association between EBP50 and 14-3-3β (Figure 10B). In addition, the T156A mutant also demonstrated a lower binding affinity to 14-3-3β (Figure 10C). These results suggest that interaction of EBP50 with 14-3-3β is regulated by its phosphorylation at T156. Beside its substrates, RSK1 itself also binds 14-3-3β, and this interaction is dependent on phosphorylation at S154 of RSK1 (Cavet et al., 2003). Interestingly, in comparison with the control mock-transduced cells, an increased binding of RSK1 with 14-3-3β was observed in EBP50-knocked down cells (Figure 10D). This implies that EBP50 may mask the binding site of 14-3-3β on RSK1, or perturb phosphorylation of RSK1 at S154 for subsequent 14-3-3β recruitment. In EBP50-knocked down cells, the RSK1 pulled down by GST-14-3-3β migrated at a slower rate compared to control cells (Figure 10D), presumably reflecting an advanced phosphorylated form of RSK1. The PDZ binding motif of RSK1 that is essential for its binding to EBP50 resides exactly at the D domain of RSK family proteins. ERK docking at the D domain is essential for phosphorylation at T573 to activate the CTKD, which in turn auto-phosphorylates RSK1 at its hydrophobic motif and NTKD for complete activation (Anjum and Blenis, 2008). EBP50 may compete with ERK for binding site at the D domain, and therefore block the subsequent phosphorylation event of RSK1 to affect its interaction with 14-3-3β.

22

3.6   Cell Cycle-dependent Phosphorylation of EBP50 is Crucial for Cell Growth

As RSK1-mediated phosphorylation of EBP50 at T156 was less in quiescent cells, but enhanced in serum- or growth factor-stimulated cells (Figures 7A and 7B), it is most probable that this phosphorylation is a cell cycle-dependent event. Indeed, EBP50 phosphorylation at T156 was not detected in cells that were synchronized at the G1-S border using double thymidine block (Figure 11A). Intriguingly, T156 phosphorylation of EBP50 was evident in cells that were released from thymidine block for 9 h, when cells were at the mitotic phase of cell cycle as marked by phosphorylation of histone H3 at S10 (Figure 11A). Cell cycle-dependent phosphorylation of EBP50 was also confirmed in HeLa cells (Figure 11B) and SW480 cells (Figure 11C) arrested at the mitotic phase. Moreover, PKC-mediated phosphorylation of EBP50 at S339-340, which regulates the affinity between the PDZ domains of EBP50 and the PDZ ligands (Chen et al., 2012; Fouassier et al., 2005; Garbett et al., 2010) was also detected in mitotic cells (Figures 11B and 11C). Therefore, the biological role of EBP50 phosphorylation during cell proliferation and growth were explored. The results from both cell proliferation assays, either the calorimetric approach (Figure 12A) or the manual counting using dye exclusion method (Figure 12B) indicated a crucial role of EBP50 phosphorylation at T156 in HeLa cells proliferation. The ability to grow in the absence of anchorage to the extracellular matrix is a hallmark of transformed cells (Paoli et al., 2013). Accordingly, HeLa cells expressing T156A mutant formed less colonies in soft agar assay compared to cells expressing wild type EBP50 (Figure 13A). Furthermore, forced nuclear expression of EBP50 by tetracycline regulatory expression markedly increased the anchorage independent growth potential on differentiated MDCK cells (Figure 13B). These *in vitro* assays suggest an essential role of EBP50 for cellular transformation. To further confirm this finding *in vivo*, tumor xenograft study was carried out, in which

23
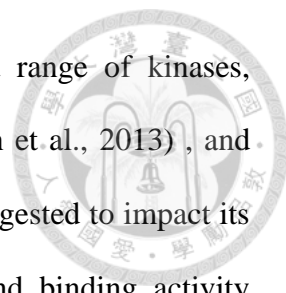
mice injected with cells expressing the phospho-resistant T156A mutant developed

smaller tumors (Figure 14) indicating that T156 phosphorylation is a critical event for

the tumor-promoting effect of EBP50.

DISCUSSION AND PERSPECTIVES

The prominent role of RSK1 in nuclear localization of EBP50 was, for the first time, uncovered by using both RNAi and biochemical approaches. RSK1 binds to EBP50 at its first PDZ domain, and mitogen-activated RSK1 phosphorylates EBP50 at T156, an event that is related to its nuclear localization. Moreover, the phosphorylation of EBP50 by RSK1 also enhances its interaction with another scaffold protein, the 14-3-3β, a molecular player that is known to regulate nuclear entry of its interacting proteins (Scholz et al., 2009; Seimiya et al., 2000); this therefore suggests two possible scenarios for the nuclear import of EBP50: (I) both phosphorylation by RSK1 and subsequent scaffolding by 14-3-3 proteins are essential, (II) EBP50 phosphorylation at T156 is sufficient (Figure 15). 14-3-3 proteins have also been implicated in nuclear transport of other proteins. 14-3-3θ (also named as 14-3-3τ) was shown to regulate nuclear accumulation of the catalytic subunit of telomerase, TERT by inhibiting its interaction with CRM1 (Seimiya et al., 2000). More recently, 14-3-3 proteins were reported to inhibit nuclear import of deleted in liver cancer 1 (DLC1) by masking its NLS (Scholz et al., 2009). Importantly, the interaction between EBP50 and RSK1 is tightly regulated by EGF stimulation (Figure 5E); and 14-3-3β, which binds to EBP50 in a T156 phosphorylation-dependent manner, also interacts with RSK1 (Figure 10D). Taken together, the results suggest that binding of RSK1 to EBP50 occurs only transiently for its kinase activity toward EBP50, which in turn creates a binding site for recruitment of 14-3-3 proteins. Since EBP50 binds to 5 out of 7 isoforms of 14-3-3 proteins, functional redundancy and isoform specificity can thus be a daunting challenging to examine if binding with 14-3-3 proteins is also a prerequisite for nuclear transport of EBP50.

25
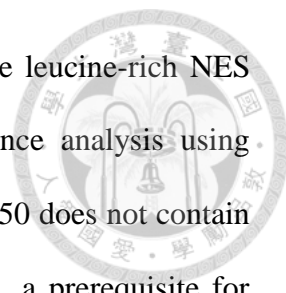
EBP50 is a highly phosphorylated protein modified by a range of kinases, including PKC (Chen et al., 2012; Garbett et al., 2010), Cdc2 (Sun et al., 2013) , and GRK6A (Hall et al., 1999). Phosphorylation of EBP50 has been suggested to impact its scaffolding function, through alteration of its oligomeric state and binding activity (Chen et al., 2012; Fouassier et al., 2005; Garbett and Bretscher, 2012). However, the integrative action of these kinases in phosphorylation of EBP50, as well as the subcellular distribution and specific cellular function of distinct phospho-forms of EBP50 remain elusive. The RSK1-mediated phosphorylation of EBP50 at T156 occurs during mitosis (Figure 11). In addition, phosphorylation of EBP50 at S339/340, the site of PKC, also happens during mitosis (Figures 11B and 11C). Furthermore, the phosphorylation of EBP50 by Cdc2 at S279 and S301 is also mitosis-phase dependent, and this phosphorylation affect its association with Pin1, a peptidyl-prolyl isomerase that its overexpression leads to G2-phase arrest of yeast and HeLa cells (Lu et al., 1996). Cdc2-mediated phosphorylation of EBP50 was shown to regulate actin cytoskeleton reorganization and plays an essential role in cytokinesis (Sun et al., 2013). Moreover, study in bovine pulmonary artery endothelial cells (BPAEC) indicates that PP2A is responsible for dephosphorylation of EBP50 at the Cdc2 phosphorylation sites during cytokinesis (Boratko et al., 2012). In addition to the phosphorylation sites of Cdc2, PP2A also responsible for dephosphorylation of EBP50 at T156, the site phosphorylated by RSK1 (Figure 7E). In interphase BPAEC, phospho-mimetic mutant of EBP50 targeted the Cdc2 phosphorylation sites was distributed in the cytoplasm while wild type protein was predominantly in the nucleus (Boratko et al., 2012). In contrast, an increased nuclear localization of T156E mutant was observed in HeLa cells compared to wild type EBP50. These findings suggest that EBP50, existing as distinct phospho-forms that are localized in different subcellular compartments, could be a signaling

nexus which finely integrates those kinases and phosphatases critically involved in the mitosis progression.

Correlation of nuclear EBP50 with cancer development and invasion was documented for hepatocellular carcinoma and colorectal carcinoma (Lin et al., 2012; Shibata et al., 2003). Previously, nuclear EBP50 was shown to promote colorectal carcinogenesis by modulating the interaction between β-catenin and TCF1 for activation of Wnt signaling pathway (Lin et al., 2012). In the present study, oncogenic RSK1, which act through its kinase activity, is shown to be the signal specific for nuclear accumulation of EBP50 in HeLa cells. The Wnt-β-catenin and Ras-ERK-RSK pathways, though acting in response to different stimuli via distinct receptors and effectors, are both important proliferative signals in tumorigenesis. The interactions between these two oncogenic signaling pathways were reported in intestinal (Jeong et al., 2012; Wang et al., 2013), prostate (Pearson et al., 2009) and pancreatic tumorigenesis (Xu et al., 2015). Study in HEK293 cells was shown that the negative regulator of Wnt-β-catenin signaling pathway, glycogen synthase 3β (GSK3β) phosphorylates H-Ras and contributes to its degradation (Jeong et al., 2012). Furthermore, Ras stabilization by aberrant activation of Wnt-β-catenin signaling was shown related to intestinal tumorigenesis (Jeong et al., 2012). The present study sheds light on an addition cross-talk between Ras-RSK1 and Wnt-β-catenin signaling which is linked by nuclear entry of EBP50.

Increased nuclear EBP50 was observed in HeLa cells treated with LMB (Figure 9B), an inhibitor of proteins nuclear export that blocks the binding of CRM1 to proteins containing the NES, through the interaction with cysteine residue of CRM1 control conserved region (Wolff et al., 1997). CRM1, a member of the family of importin β-related nuclear transport receptor, has been reported to export certain type of RNA

(Brennan et al., 2000; Popa et al., 2002), and proteins that bear the leucine-rich NES (Ossareh-Nazari et al., 1997) from the nucleus. However, sequence analysis using NESbase 1.0 search program (la Cour et al., 2003) showed that EBP50 does not contain the classical leucine-rich NES for physical interaction with CRM1, a prerequisite for CRM1 cargo proteins. This implies that EBP50 could possibly be exported from the nucleus through a cryptic binding with CRM1 or alternatively through some interacting partners of EBP50, which contain the leucine-rich NES such as β-catenin (Ki et al., 2008), EGFR (Lo et al., 2006) and GRK6A (Johnson et al., 2013).

Dual function proteins, such as EBP50, may execute essential physiological functions at one particular cellular compartment, while also play unwanted pathological roles when they wander to another subcellular localization. Thus, therapeutic approach targeting directly at diminishing such versatile proteins might compromise their normal physiological function; however, prevention of their mislocalization would be an ideal option to preserve essential cellular functions. This study not only deciphers the molecular mechanism for nuclear localization of EBP50, a mislocalization that contributes to its pro-proliferative role, but also identifies RSK1 as potential target to prevent aberrant subcellular trafficking of EBP50, a phenomenon commonly occurring in advanced malignancies.
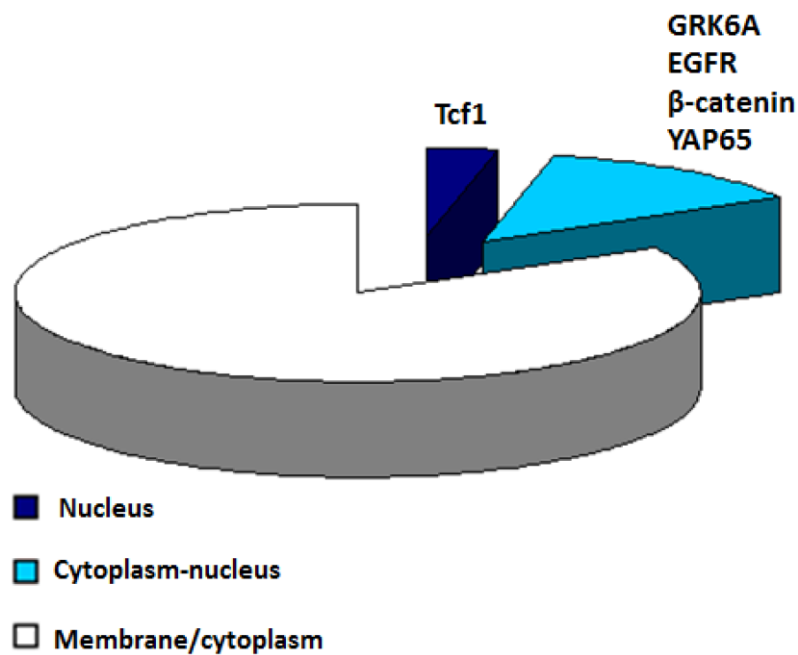
Figure 1 **Literature-based classification of interacting partners of EBP50 according to their subcellular localization.** EBP50 interacts physically with PDZ motif-containing membrane and cytoplasmic proteins (Shenolikar et al., 2004). EBP50 was also demonstrated to interact with proteins that shuttle between cytoplasm and nucleus, including GRK6A (Hall et al., 1999), EGFR (Claperon et al., 2012), β-catenin (Shibata et al., 2003) and YAP65 (Mohler et al., 1999), as well as the nucleus-localized Wnt responsive transcription factor TCF1 (Lin et al., 2012).
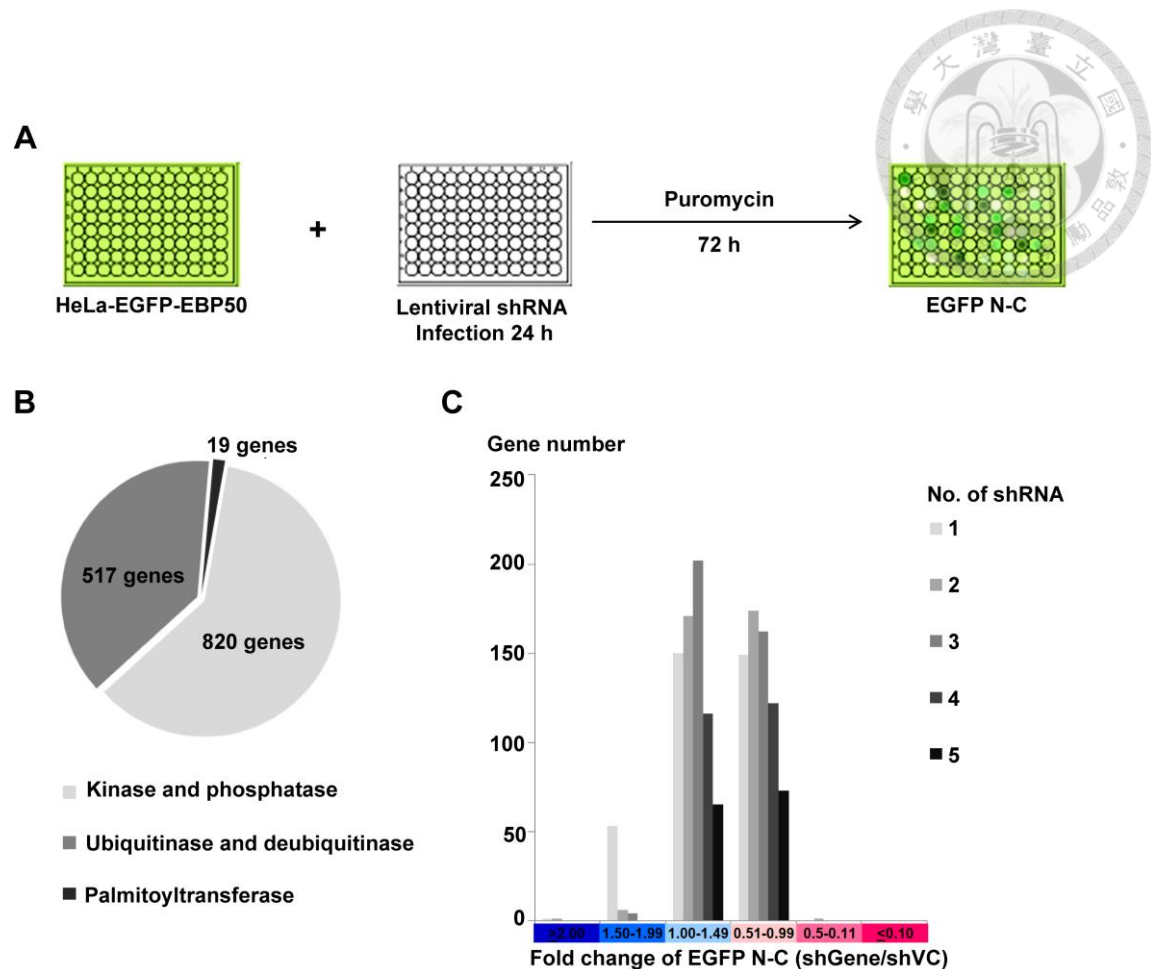
Figure 2   A RNAi screening aimed for genes regulating the nucleocytoplasmic shuttling of EBP50. (**A**) Schematic diagram of the RNAi screening that was subsequently coupled with image analysis to search for genes involved in nucleocytoplasmic transport of EBP50. (**B**) Totally 1356 genes composed of 3 major enzymatic subclasses responsible for protein phosphorylation, ubiquitination, and palmitoylation were screened for their potential effects on the nucleocytoplasmic shuttling of EBP50. (**C**) The result of the screening after normalization with the nuclear and cytosolic difference (N-C) of EGFP signals observed in mock-transduced cells (shVC) were presented according to the distribution of shRNA hits in the designated categories for each gene.

Fold change EGFP N-C (shGene/shVC)
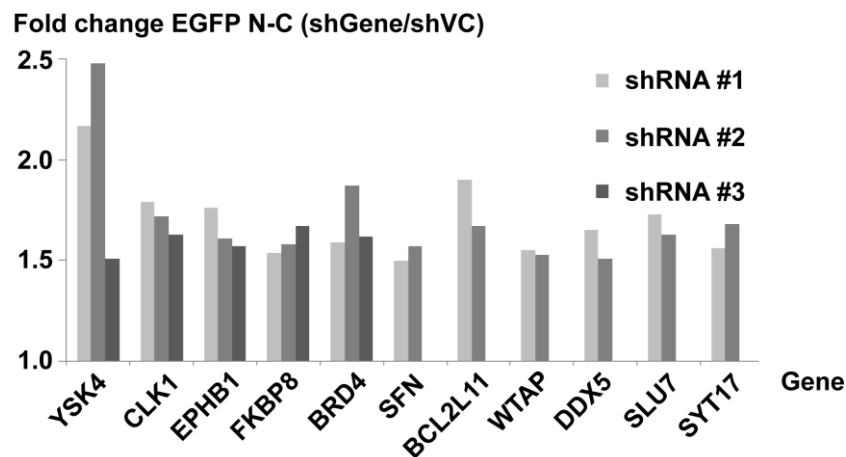
Figure 3   The potential regulators in nuclear export of EBP50 identified from RNAi screening. A total of 11 genes of the human kinase shRNA library were identified as the potential regulator in nuclear export of EBP50 as knockdown of the candidate gene each resulted in increase of nuclear EBP50.
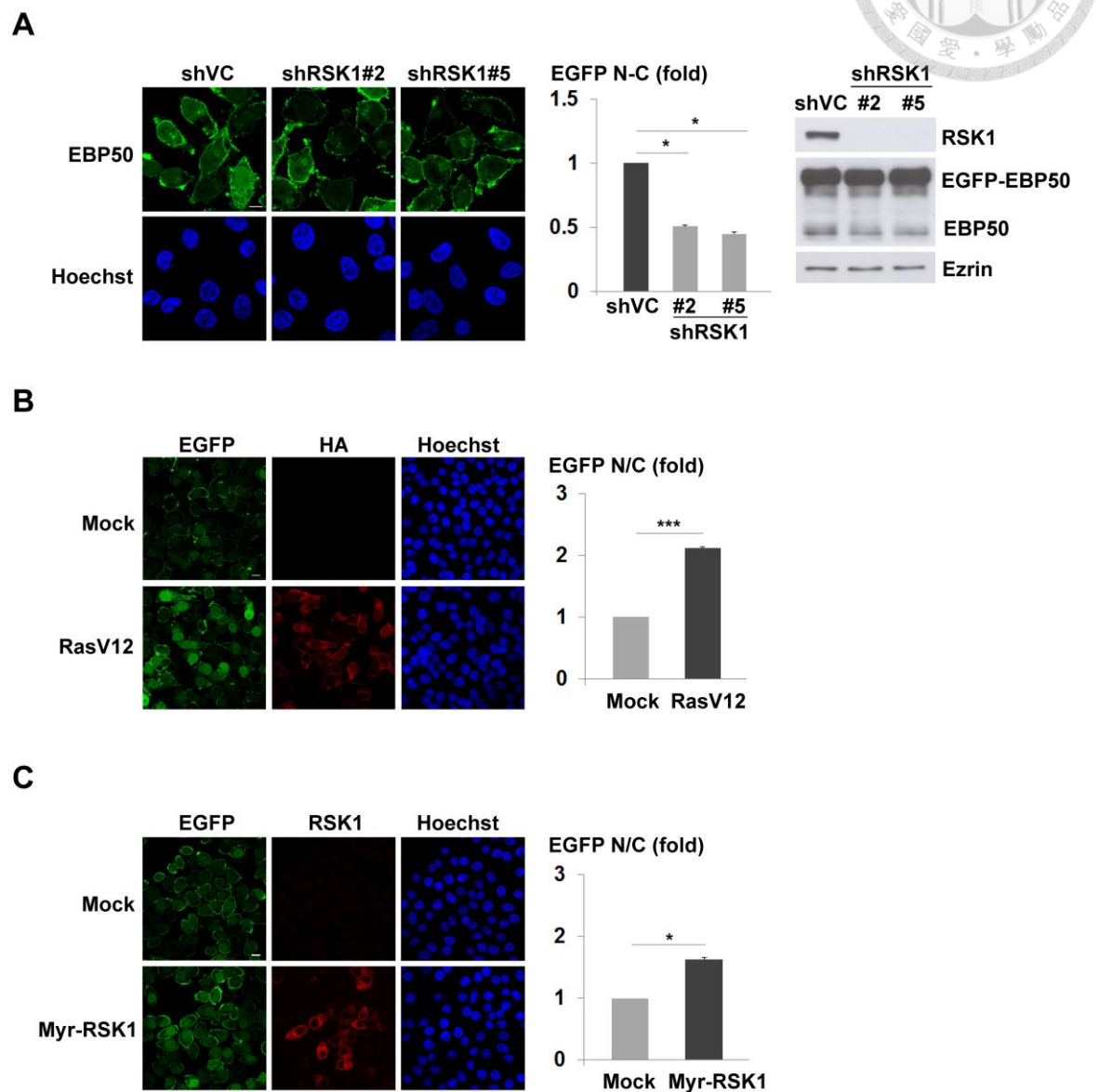
Figure 4   Ras-RSK1 signaling regulates nuclear localization of EBP50.

See next page for legend.

Figure 4 **Ras-RSK1 signaling regulates nuclear localization of EBP50.** (**A**) HeLa-EGFP-EBP50 cells were separately infected with two independent clones of lentiviruses expressing shRNAs against RSK1. Transduced cells were processed for images analysis and N-C difference of EGFP signal was measured. Western blotting analysis demonstrated the knockdown efficiency of RSK1 in these cells (right panel). Ezrin was examined as a loading control. HeLa-EGFP-EBP50 cells were transfected with a plasmid encoding HA-tagged constitutive active Ras (HA-RasV12) (**B**), constitutive active RSK1 (Myr-RSK1) (**C**), or the empty vector (mock). The cells were then fixed at 24 h post-transfection, stained with anti-HA (**B**) or anti-RSK1 antibody (**C**), and then images were captured and N/C ratio of EGFP signal were quantified. Scale bar: 10 μm. Data are means $\pm$ SEM of 150-200 cells. * $p < 0.05$, *** $p < 0.001$, Student's *t*-test.
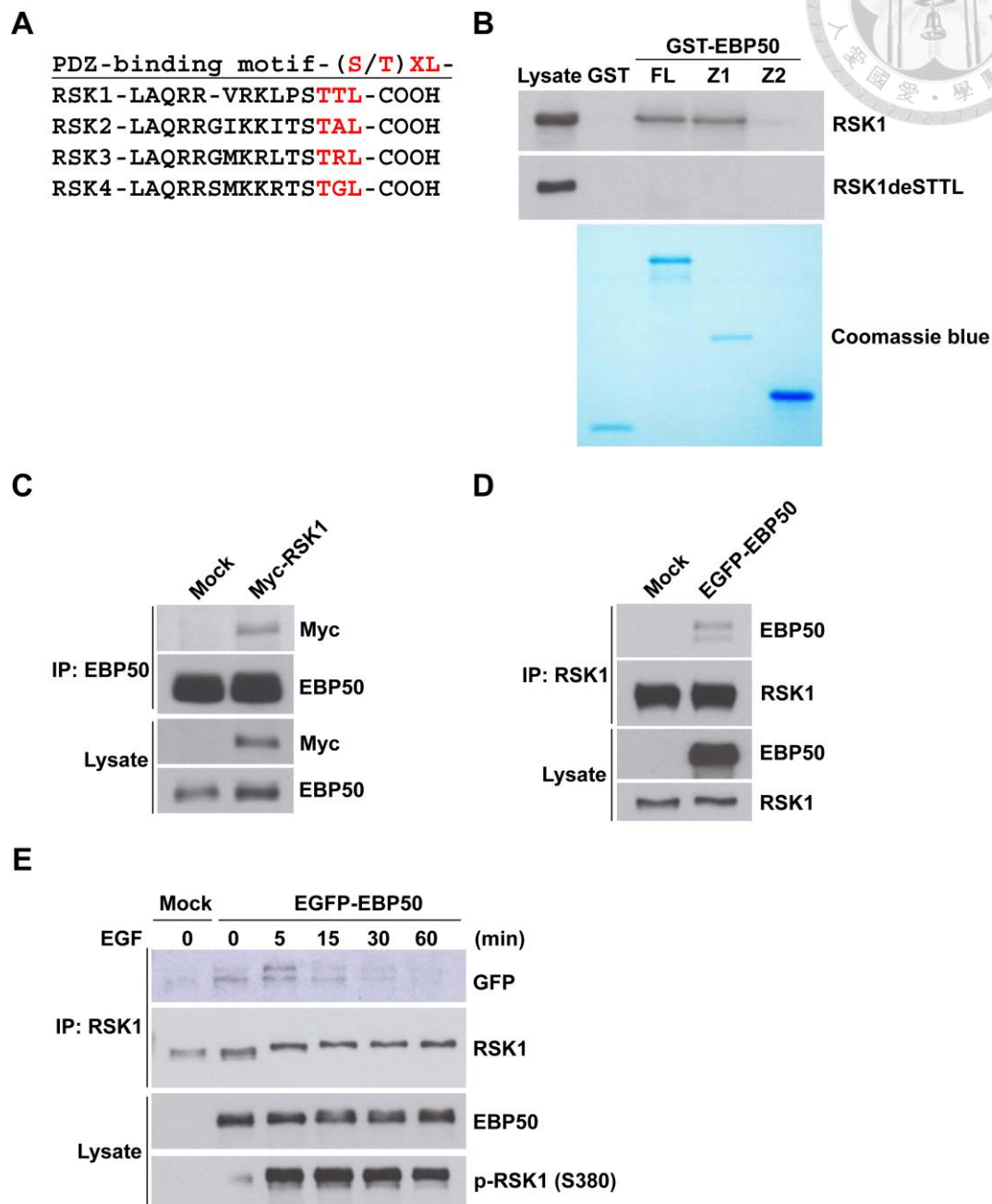
A

```
PDZ-binding motif-(S/T)XL-
RSK1-LAQRR-VRKLPSTTL-COOH
RSK2-LAQRRGIKKITSTAL-COOH
RSK3-LAQRRGMKRLTSTRL-COOH
RSK4-LAQRRSMKKRTSTGL-COOH
```

B

GST-EBP50
Lysate GST | FL | Z1 | Z2

RSK1

RSK1deSTTL

Coomassie blue

C

IP: EBP50

Myc
EBP50

Lysate

Myc
EBP50

D

IP: RSK1

EBP50
RSK1

Lysate

EBP50
RSK1

E

Mock | EGFP-EBP50
EGF 0 | 0 5 15 30 60 (min)

GFP

IP: RSK1

RSK1

EBP50

Lysate

p-RSK1 (S380)

Figure 5 **RSK1 binds to EBP50 through a PDZ binding motif and PDZ domain interaction which is subjective to signaling regulation.** See next page for legend.
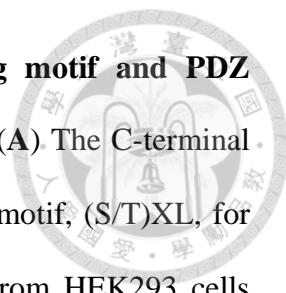
Figure 5   RSK1 binds to EBP50 through a PDZ binding motif and PDZ domain interaction which is subjective to signaling regulation. (**A**) The C-terminal sequences of all four RSK isoforms contain putative PDZ binding motif, (S/T)XL, for the tandem repeated PDZ domains of EBP50. (**B**) Cell lysates from HEK293 cells transiently expressing Myc-tagged full length RSK1 (RSK1) or a PDZ binding motif deletion mutant (RSK1deSTTL) were subjected for in vitro pull-down assay with GST-fused full length (FL), first PDZ domain (Z1) or second PDZ domain (Z2) EBP50 construct. The pulled down materials were separated by SDS-PAGE and analysed by Western blotting using anti-Myc antibody. The coomassie blue-stained gel showed the expression and comparable loading of each recombinant protein used in the assay. (**C**) The cellular lysates from HeLa cells that were transfected with Myc-RSK1 or the empty vector were immunoprecipitated with EBP50 antibody and the co-immunoprecipiated RSK1 was analysed by Western blotting using anti-Myc antibody. (**D**) HeLa cells were transfected with EGFP-EBP50 or an empty vector. Then, endogenous RSK1 was immunoprecipitated from the cell lysates and the immunoprecipiated materials were analysed by Western blotting using anti-EBP50 antibody. (**E**) EBP50-knocked down HeLa cells that stably re-expressed EGFP-EBP50 or empty vector were serum starved for 20 h, and stimulated with EGF (50 ng/ml) for the indicated intervals. Then, RSK1 was immunoprecipitated from the harvested lysates followed by Western blotting using anti-GFP antibody.

A

RSK phosphorylation motif-RXRXXpS/T-
EBP50 Human -EL**R**P**R**LC**T**^{156}MKK-
         Mouse -EL**R**P**R**LC**T**^{153}MKK-
         Rat   -EL**R**P**R**LC**T**^{155}MKK-

B

Phosphopeptide for immunization
T156NP:LRPRLS(T)MKKGPSC
T156P :LRPRLS(pT)MKKGPSC

C
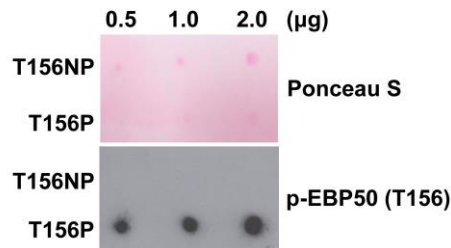
Figure 6   Generation and analysis of anti-phospho-EBP50 (T156) antibody. (A) Mammalian EBP50 conserves an RXRXXpS/T sequence which matched with the consensus phosphorylation motif of RSK1 substrates. (**B**) The amino acids sequence of synthetic phosphopeptide (T156P) used to generate site and phosphorylation state-specific antibody for EBP50. A control peptide (T156NP) was also synthesized in which T156 was not phosphorylated. (**C**) Dot blot analysis to assess the production of a phospho-specific antibody, p-EBP50 (T156), for application in studies on phosphorylation of EBP50 at T156.
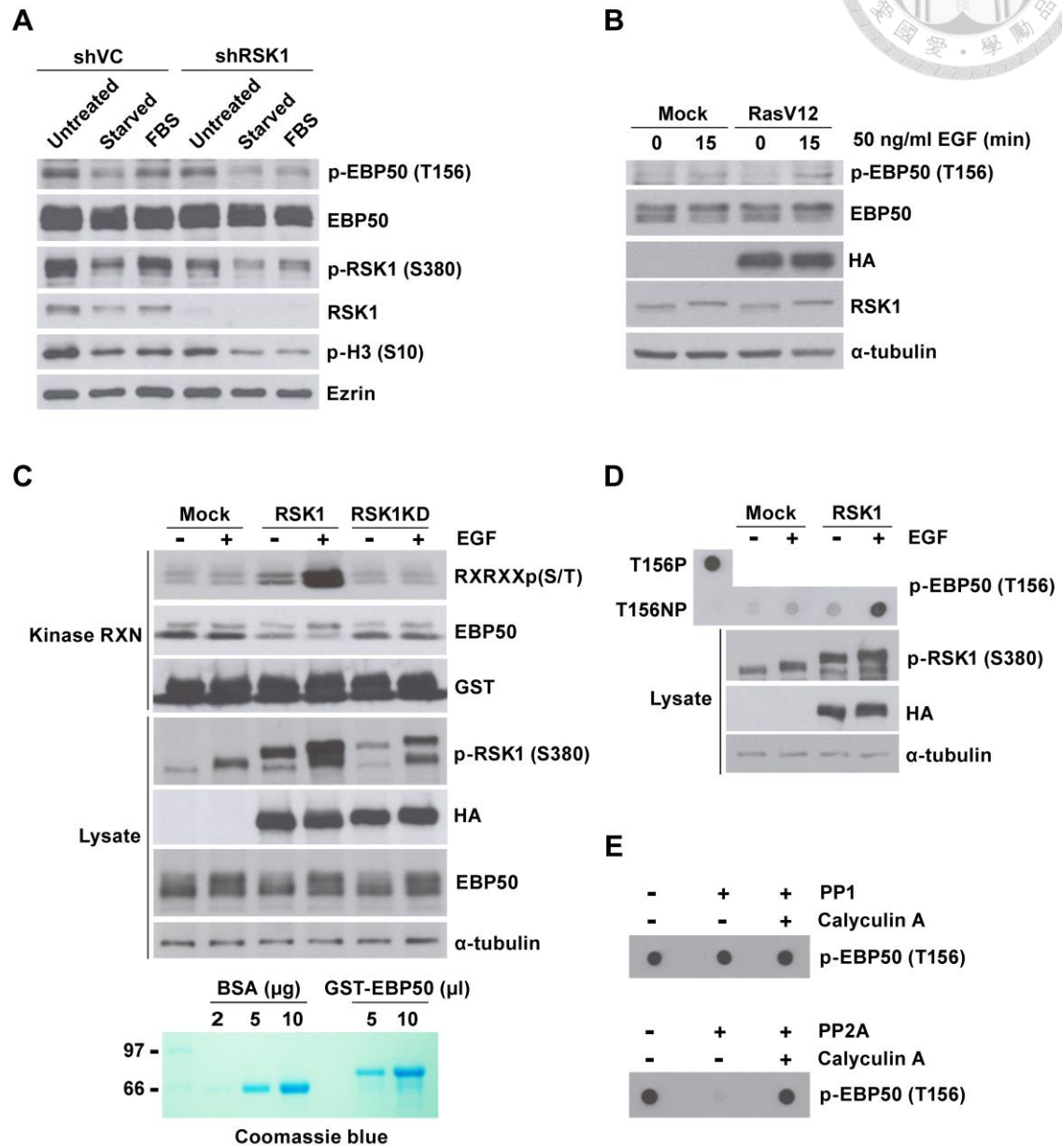
Figure 7   RSK1 phosphorylates EBP50 at T156 within a consensus RXRXXpS/T motif. See next page for legend.

Figure 7 **RSK1 phosphorylates EBP50 at T156 within a consensus RXRXXpS/T motif.** (**A**) RSK1-knocked down HeLa cells (shRSK1) or mock-transduced cells (shVC) were grown in complete media (untreated), serum-starved, or re-stimulated with 10% (v/v) serum for 7 h (FBS). Phosphorylation of EBP50 was analysed by Western blotting using the phospho-T156 antibody. In parallel, the samples were assayed for knock down efficiency and activation of RSK1 using anti-RSK1 antibody and phospho-S380 antibody, respectively. (**B**) HEK293 cells were transfected with a HA-RasV12 expressing plasmid or an empty vector. The cells were serum starved for 16 h, and then simulated with EGF for 15 min. Phosphorylation of EBP50 was assayed by Western blotting using phospho-T156 antibody. (**C**) HEK293 cells were transfected with either HA-tagged wild type RSK1 (RSK1), its kinase dead mutant (RSK1KD), or an empty vector, serum starved for 16 h, and stimulated with 50 ng/ml of EGF for 15 min. The immunoprecipitated RSK1 was incubated with 5 µl purified GST-EBP50 in a kinase reaction buffer containing 0.5 mM ATP at 37°C for 30 min. Phosphorylation of EBP50 was analysed by Western blotting using an antibody recognizing the RXRXXpS/T motif. (**D**) HEK293 cells were transfected with HA-RSK1 or empty vector, serum starved for 16 h, and stimulated with 50 ng/ml of EGF for 15 min. The immunoprecipitated RSK1 using anti-HA antibody was incubated with synthetic peptide of EBP50 (T156NP) in a kinase reaction buffer containing 0.5 mM ATP at 37°C for 30 min. The samples were then processed for dot blot analysis using phospho-T156 antibody. Synthetic phosphopeptide of EBP50 (T156P) was included as a positive control. (**E**) Purified PP1 (upper panel) or PP2A (lower panel) was incubated with synthetic phosphopeptide of EBP50 in the presence or absence of Calyculin A at 30°C for 30 min. The samples were then processed for dot blot analysis using phospho-T156 antibody. Ezrin or α-tubulin was examined as a loading control.
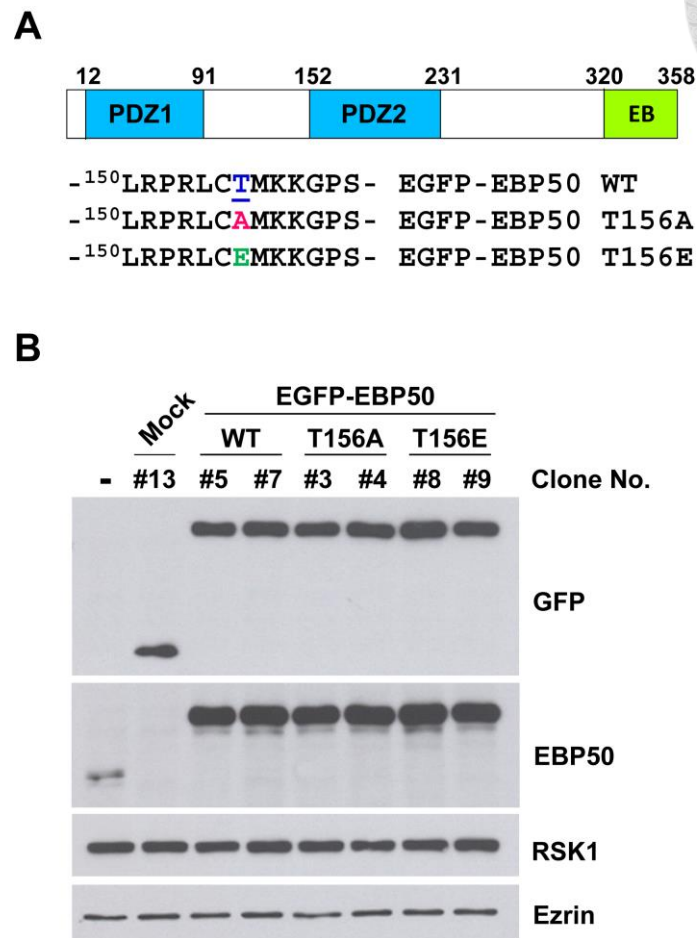
Figure 8   Endogenous EBP50-knocked down HeLa cells stably re-expressing phospho-mutants of EBP50. (**A**) Schematic diagram of phospho-mutants of human EBP50 (WT) in which threonine residue at position 156 within the RXRXXpS/T motif were replaced with either alanine (T156A) or glutamate (T156E) as indicated. (**B**) Western blotting analysis using both GFP and EBP50 antibodies to detect both exogenous and endogenous protein expression levels in HeLa clones stably re-expressing EGFP-tagged wild type EBP50 and its phospho-mutants at T156. Ezrin and RSK1 were examined as the loading controls.
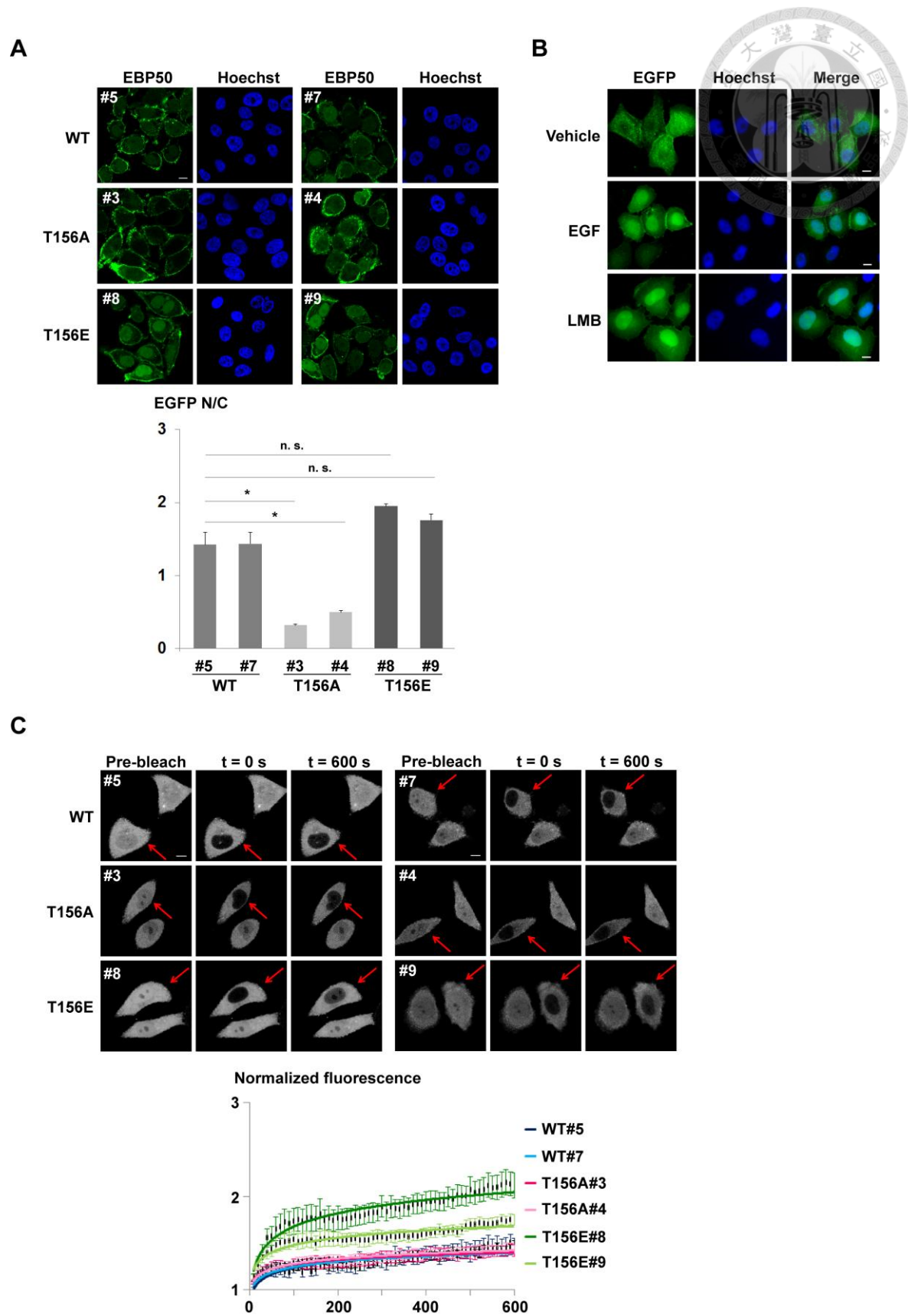
Figure 9　　**Phosphorylation of EBP50 at T156 is related to increased nuclear localization.** See next page for legend.

Figure 9　　Phosphorylation of EBP50 at T156 is related to increased nuclear localization. (**A**) Immunofluorescence staining to analyse subcellular distribution of EBP50 and its phospho-mutants in cells grown in complete media. Quantitative data are means $\pm$ SEM of 50-60 cells. * $p < 0.05$, n.s. not significant, Student's *t*-test. (**B**) HeLa cells transiently expressing EGFP-EBP50 was serum-starved before being treated with EGF or LMB. (**C**) Photobleaching nuclear import assay on phospho-mutants of EBP50. Fluorescence images of typical cells from each clones at pre- or post-bleach times and at experimental end points. Quantitative data of the indicated photobleached-cells (red arrow) for recovery of fluorescence are means $\pm$ SEM of 14 cells for each clone. Scale bar: 10 μm.
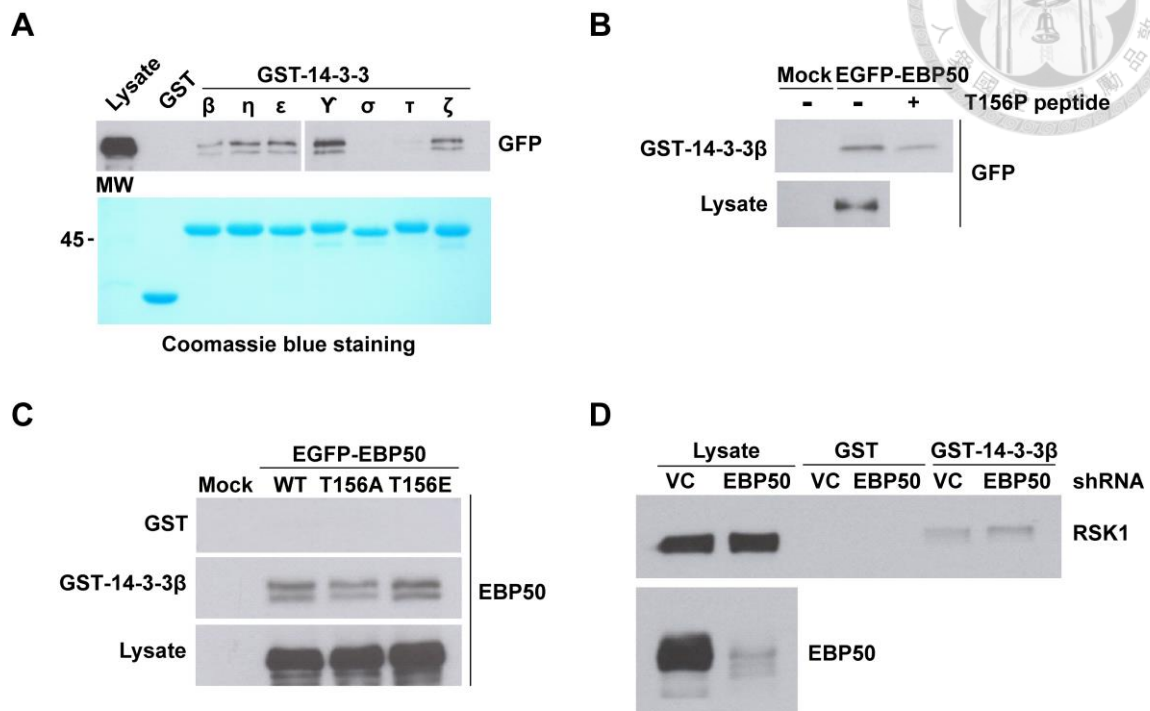
Figure 10   Phosphorylation of EBP50 at T156 promotes its binding to 14-3-3β.

(**A**) Cell lysates prepared from HEK293 cells transiently expressing EGFP-EBP50 were subjected for *in vitro* pull-down assay with various isoforms of GST-14-3-3 proteins. The purity and quantity of each fusion protein used in the assay was shown by the coomassie-stained gel. The pulled down materials were separated by SDS-PAGE and analysed by Western blotting using anti-GFP antibody. (**B**) Cell lysates prepared from HEK293 cells transiently expressing EGFP-EBP50 were subjected for pull-down assay with GST-14-3-3β in the presence (+) or absence (-) of synthetic phosphopeptide T156P. (**C**) GST pull-down assay to test the ability of phosho-mutants of EBP50 to bind 14-3-3β in HEK293 cells transiently expressing the indicated constructs. (**D**) Interaction between RSK1 and 14-3-3β that investigated in EBP50-knocked down HeLa cells and the mock-transduced (VC) cells by GST pull-down assay.
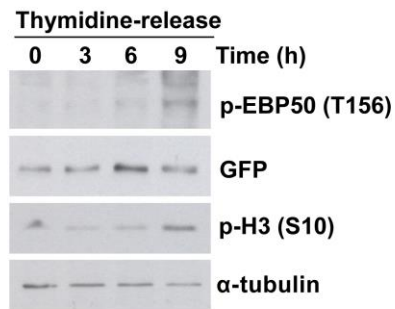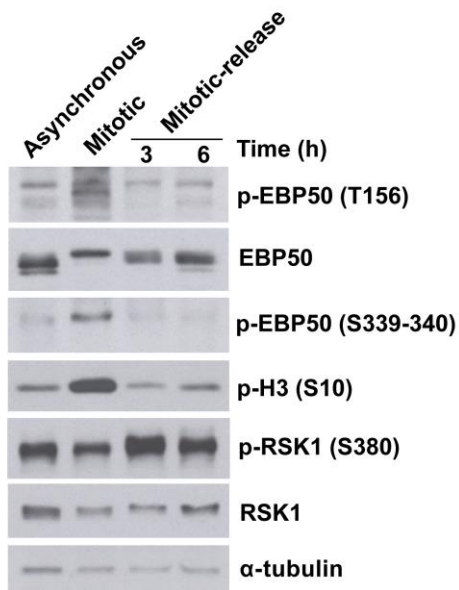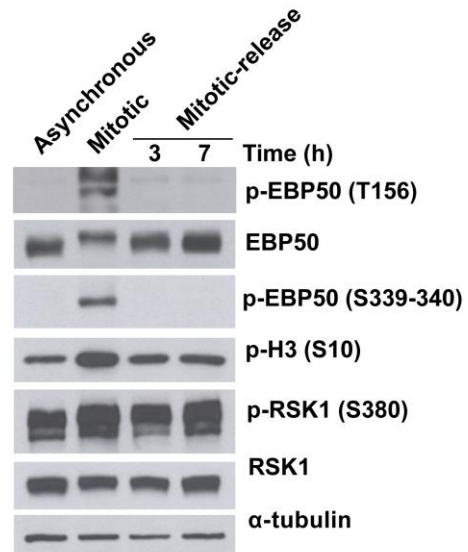
Figure 11   Cell cycle-dependent phosphorylation of EBP50. (**A**) HeLa cells expressing EGFP-EBP50 were synchronize at G1-S border using double thymidine block and released from the block for 0, 3, 6, or 9 h. Phosphorylation of EBP50 was assayed by Western blotting using phospho-T156 antibody. Phosphorylation of histone H3 at S10 was used as the mitotic marker. HeLa cells (**B**) or SW480 cells (**C**) were synchronize at mitotic phase using thymidine-nocodazole block (mitotic) and released from the block (mitotic release) for 6 h (**B**) or 7 h (**C**). Phosphorylation of EBP50 was assayed by Western blotting using phospho-T156 and phospho-S339-340 antibodies.
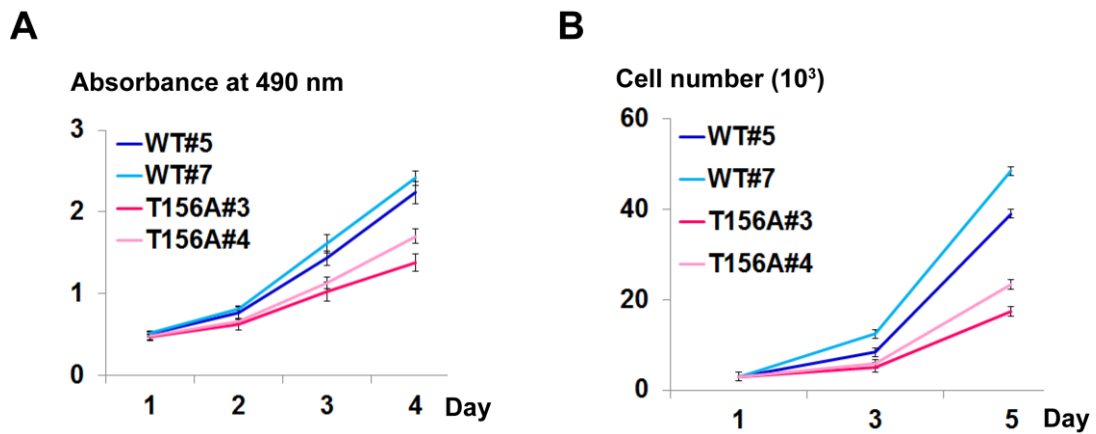
Figure 12   **Phosphorylation of EBP50 at T156 is crucial for cell proliferation.** (**A**) Cell proliferation assayed using MTS reagent. Data are means ± SEM of 3 independent experiments. (**B**) Trypan blue exclusion analysis to examine the growth of HeLa cells expressing wild type and T156A mutant of EBP50; each with two independent stable clones.
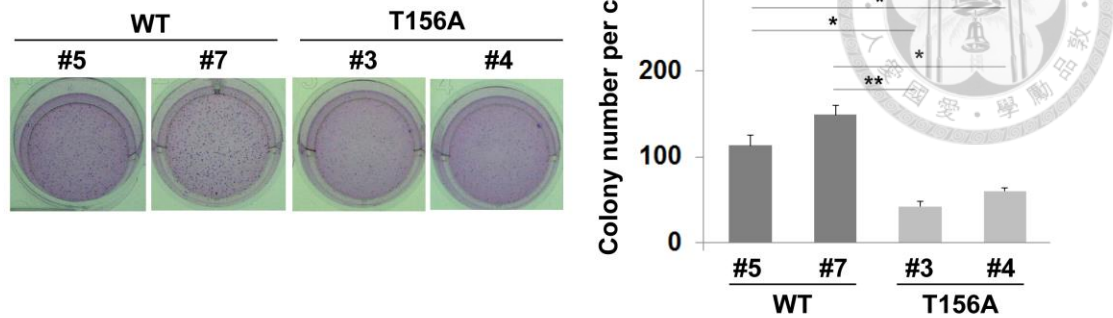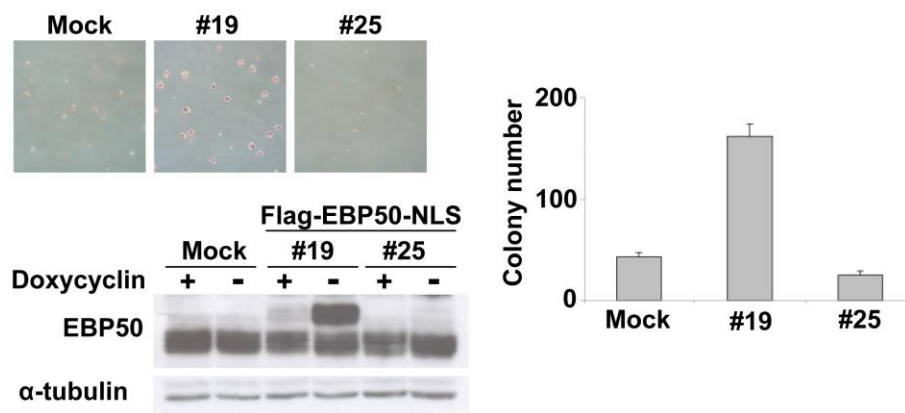
Figure 13 **Phosphorylation of EBP50 at T156 is crucial for *in vitro* cell transformation.** (**A**) Photos and counting of cresyl violet-stained colonies formed in soft agar assay. Data are means $\pm$ SEM. * $p < 0.05$, ** $p < 0.01$, Student's *t*-test. (**B**) Soft agar assay for MDCK cells stably expressing amino terminally Flag-tagged and carboxyl terminally NLS-fused EBP50 under tetracycline-repressible system. Western blotting analysis demonstrated one stable clone (#19) expressed comparable level of NLS-fused EBP50 to endogenous EBP50 when doxycycline was removed. Another stable clone (#25) which failed to express the exogenous protein and a mock transfectant were used as negative controls when all cell lines were cultured in the absence of doxycycline for soft agar assays.
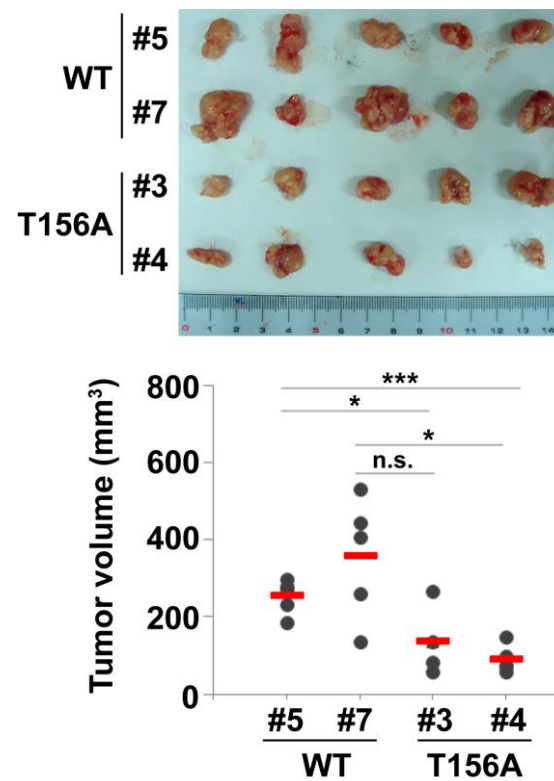
Figure 14   Phosphorylation of EBP50 at T156 is crucial for *in vivo* cell transformation. HeLa cells expressing wild type and T156A mutant of EBP50 were injected subcutaneously at the dorsal sites of 8 weeks old NOD/SCID mice. The tumor sizes were measured 4 weeks after injection.
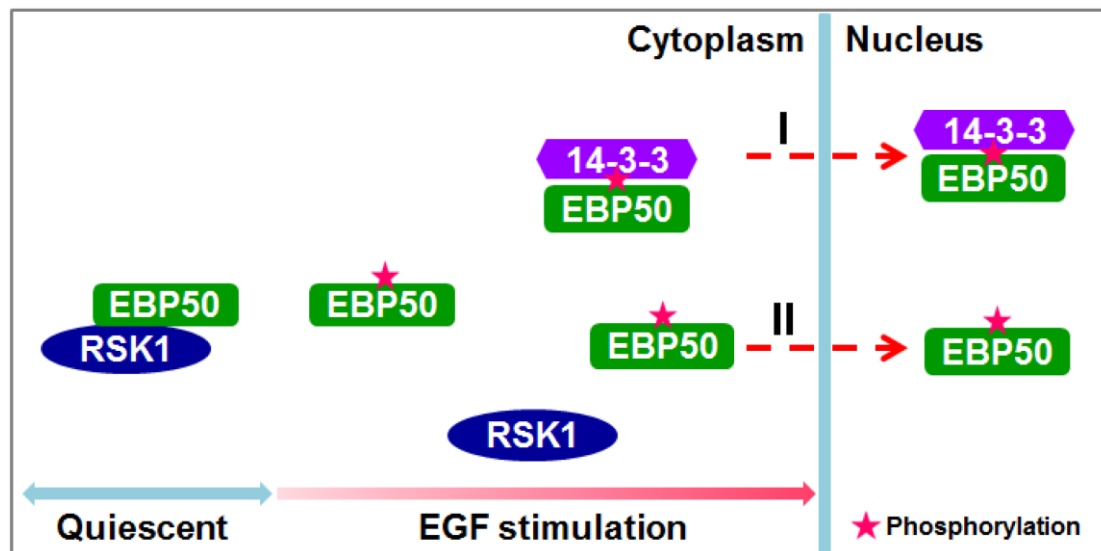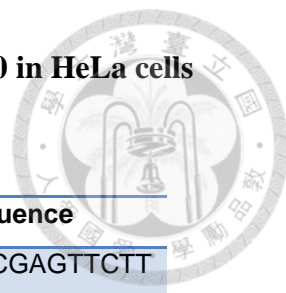
Figure 15　　**Schematic diagrams showing the role of RSK1 and 14-3-3β in nuclear accumulation of EBP50.** RSK1 binds to EBP50 and phosphorylates it at T156 under regulation of EGF. The phosphorylation of EBP50 at T156 is related to its nuclear localization, and enhances its physical interaction with 14-3-3β. Therefore, two possible scenarios were proposed for the nuclear import of EBP50: (I) both phosphorylation by RSK1 and subsequent scaffolding by 14-3-3 proteins are essential, (II) EBP50 phosphorylation at T156 is sufficient.

Table 1   **The sequence of primers used to generate plasmid constructs**

Plasmid	ID	Sequence
pEGFP-EBP50	100	TATGTTCTCGAGAAATGAGCGCGGACGCAGCGG
	142	GGATCCTCAGAGGTTGCTGAAGAGTTCGT
pEGFP-EBP50T156A	100	TATGTTCTCGAGAAATGAGCGCGGACGCAGCGG
	142	GGATCCTCAGAGGTTGCTGAAGAGTTCGT
	179	GGCTCTGTGCCATGAAGAAGGGCCC
	148	TCTTCATGGCACAGAGCCGAGGCCG
pEGFP-EBP50T156E	100	TATGTTCTCGAGAAATGAGCGCGGACGCAGCGG
	142	GGATCCTCAGAGGTTGCTGAAGAGTTCGT
	181	GGCTCTGTGAGATGAAGAAGGGCCC
	150	TCTTCATCTCACAGAGCCGAGGCCG
shRNA resistant EBP50	100	TATGTTCTCGAGAAATGAGCGCGGACGCAGCGG
	142	GGATCCTCAGAGGTTGCTGAAGAGTTCGT
	183	TCGCGAGACCGATGAATTTTTTAAGAAATGCAGAGTGATC
	152	AAAAAATTCATCGGTCTCGCGATCCACCACCAGCAGCTTG
shRNA resistant T156A	100	TATGTTCTCGAGAAATGAGCGCGGACGCAGCGG
	142	GGATCCTCAGAGGTTGCTGAAGAGTTCGT
	179	GGCTCTGTGCCATGAAGAAGGGCCC
	148	TCTTCATGGCACAGAGCCGAGGCCG
	183	TCGCGAGACCGATGAATTTTTTAAGAAATGCAGAGTGATC
	152	AAAAAATTCATCGGTCTCGCGATCCACCACCAGCAGCTTG
shRNA resistant T156E	100	TATGTTCTCGAGAAATGAGCGCGGACGCAGCGG
	142	GGATCCTCAGAGGTTGCTGAAGAGTTCGT
	181	GGCTCTGTGAGATGAAGAAGGGCCC
	150	TCTTCATCTCACAGAGCCGAGGCCG
	183	TCGCGAGACCGATGAATTTTTTAAGAAATGCAGAGTGATC
	152	AAAAAATTCATCGGTCTCGCGATCCACCACCAGCAGCTTG

Table 2   The sequence of shRNA used to kncokdown EBP50 in HeLa cells

Gene Symbol	Accession No.	shRNA Target Sequence
SLC9A3R1 (EBP50)	NM_004252	CAGGGAAACTGACGAGTTCTT

Table 3   **The sequence of shRNA used to kncokdown RSK1 in HeLa cells**

shRNA ID	Target Sequence	Region
shRSK1#1	AGCGATTCACTGTATAAACTT	3'UTR
shRSK1#2	GCTCTATCTCATTCTGGACTT	CDS
shRSK1#3	GAAGGAGACCATGACACTGAT	CDS
shRSK1#4	ACACAGTTTCAGAGACAGCCA	CDS
shRSK1#5	GACCATGACACTGATTCTGAA	CDS

REFERENCES

Anjum, R., and Blenis, J. (2008). The RSK family of kinases: emerging roles in cellular signalling. Nature reviews Molecular cell biology *9*, 747-758.

Bakiri, L., Reschke, M.O., Gefroh, H.A., Idarraga, M.H., Polzer, K., Zenz, R., Schett, G., and Wagner, E.F. (2011). Functions of Fos phosphorylation in bone homeostasis, cytokine response and tumourigenesis. Oncogene *30*, 1506-1517.

Bonni, A., Brunet, A., West, A.E., Datta, S.R., Takasu, M.A., and Greenberg, M.E. (1999). Cell survival promoted by the Ras-MAPK signaling pathway by transcription-dependent and -independent mechanisms. Science *286*, 1358-1362.

Boratko, A., Gergely, P., and Csortos, C. (2012). Cell cycle dependent association of EBP50 with protein phosphatase 2A in endothelial cells. PloS one *7*, e35595.

Brennan, C.M., Gallouzi, I.E., and Steitz, J.A. (2000). Protein ligands to HuR modulate its interaction with target mRNAs in vivo. The Journal of cell biology *151*, 1-14.

Cavet, M.E., Lehoux, S., and Berk, B.C. (2003). 14-3-3beta is a p90 ribosomal S6 kinase (RSK) isoform 1-binding protein that negatively regulates RSK kinase activity. The Journal of biological chemistry *278*, 18376-18383.

Chen, J.Y., Lin, Y.Y., and Jou, T.S. (2012). Phosphorylation of EBP50 negatively regulates beta-PIX-dependent Rac1 activity in anoikis. Cell death and differentiation *19*, 1027-1037.

Chen, R.H., Abate, C., and Blenis, J. (1993). Phosphorylation of the c-Fos transrepression domain by mitogen-activated protein kinase and 90-kDa ribosomal S6 kinase. Proceedings of the National Academy of Sciences of the United States of America *90*, 10952-10956.

Chen, R.H., Sarnecki, C., and Blenis, J. (1992). Nuclear localization and regulation of erk- and rsk-encoded protein kinases. Molecular and cellular biology *12*, 915-927.

Claperon, A., Guedj, N., Mergey, M., Vignjevic, D., Desbois-Mouthon, C., Boissan, M., Saubamea, B., Paradis, V., Housset, C., and Fouassier, L. (2012). Loss of EBP50 stimulates EGFR activity to induce EMT phenotypic features in biliary cancer cells. Oncogene *31*, 1376-1388.

Dehan, E., Bassermann, F., Guardavaccaro, D., Vasiliver-Shamis, G., Cohen, M., Lowes, K.N., Dustin, M., Huang, D.C., Taunton, J., and Pagano, M. (2009). betaTrCP- and Rsk1/2-mediated degradation of BimEL inhibits apoptosis. Molecular cell *33*, 109-116.

Doehn, U., Hauge, C., Frank, S.R., Jensen, C.J., Duda, K., Nielsen, J.V., Cohen, M.S., Johansen, J.V., Winther, B.R., Lund, L.R.*, et al.* (2009). RSK is a principal effector of the RAS-ERK pathway for eliciting a coordinate promotile/invasive gene program and phenotype in epithelial cells. Molecular cell *35*, 511-522.

Drenan, R.M., Doupnik, C.A., Boyle, M.P., Muglia, L.J., Huettner, J.E., Linder, M.E., and Blumer, K.J. (2005). Palmitoylation regulates plasma membrane-nuclear shuttling of R7BP, a novel membrane anchor for the RGS7 family. The Journal of cell biology *169*, 623-633.

Esteller, M., Cordon-Cardo, C., Corn, P.G., Meltzer, S.J., Pohar, K.S., Watkins, D.N., Capella, G., Peinado, M.A., Matias-Guiu, X., Prat, J.*, et al.* (2001). p14ARF silencing by promoter hypermethylation mediates abnormal intracellular localization of MDM2. Cancer research *61*, 2816-2821.

Fehon, R.G., McClatchey, A.I., and Bretscher, A. (2010). Organizing the cell cortex: the role of ERM proteins. Nature reviews Molecular cell biology *11*, 276-287.

Fouassier, L., Duan, C.Y., Feranchak, A.P., Yun, C.H., Sutherland, E., Simon, F., Fitz, J.G., and Doctor, R.B. (2001). Ezrin-radixin-moesin-binding phosphoprotein 50 is expressed at the apical membrane of rat liver epithelia. Hepatology *33*, 166-176.

Fouassier, L., Nichols, M.T., Gidey, E., McWilliams, R.R., Robin, H., Finnigan, C., Howell, K.E., Housset, C., and Doctor, R.B. (2005). Protein kinase C regulates the phosphorylation and oligomerization of ERM binding phosphoprotein 50. Experimental cell research *306*, 264-273.

Fouassier, L., Rosenberg, P., Mergey, M., Saubamea, B., Claperon, A., Kinnman, N., Chignard, N., Jacobsson-Ekman, G., Strandvik, B., Rey, C.*, et al.* (2009). Ezrin-radixin-moesin-binding phosphoprotein (EBP50), an estrogen-inducible scaffold protein, contributes to biliary epithelial cell proliferation. The American journal of pathology *174*, 869-880.

Galan, J.A., Geraghty, K.M., Lavoie, G., Kanshin, E., Tcherkezian, J., Calabrese, V., Jeschke, G.R., Turk, B.E., Ballif, B.A., Blenis, J.*, et al.* (2014). Phosphoproteomic analysis identifies the tumor suppressor PDCD4 as a RSK substrate negatively regulated by 14-3-3. Proceedings of the National Academy of Sciences of the United States of America *111*, E2918-2927.

Garbett, D., and Bretscher, A. (2012). PDZ interactions regulate rapid turnover of the scaffolding protein EBP50 in microvilli. The Journal of cell biology *198*, 195-203.

Garbett, D., LaLonde, D.P., and Bretscher, A. (2010). The scaffolding protein EBP50 regulates microvillar assembly in a phosphorylation-dependent manner. The Journal of cell biology *191*, 397-413.

Georgescu, M.M., Cote, G., Agarwal, N.K., and White, C.L., 3rd (2014). NHERF1/EBP50 controls morphogenesis of 3D colonic glands by stabilizing PTEN and ezrin-radixin-moesin proteins at the apical membrane. Neoplasia *16*, 365-374 e361-362.

Hall, R.A., Spurney, R.F., Premont, R.T., Rahman, N., Blitzer, J.T., Pitcher, J.A., and Lefkowitz, R.J. (1999). G protein-coupled receptor kinase 6A phosphorylates the Na(+)/H(+) exchanger regulatory factor via a PDZ domain-mediated interaction. J Biol Chem *274*, 24328-24334.

Hanono, A., Garbett, D., Reczek, D., Chambers, D.N., and Bretscher, A. (2006). EPI64 regulates microvillar subdomains and structure. The Journal of cell biology *175*, 803-813.

Harley, V.R., Layfield, S., Mitchell, C.L., Forwood, J.K., John, A.P., Briggs, L.J., McDowall, S.G., and Jans, D.A. (2003). Defective importin beta recognition and nuclear import of the sex-determining factor SRY are associated with XY sex-reversing mutations. Proceedings of the National Academy of Sciences of the United States of America *100*, 7045-7050.

Huang, L., Ren, J., Chen, D., Li, Y., Kharbanda, S., and Kufe, D. (2003). MUC1 cytoplasmic domain coactivates Wnt target gene transcription and confers transformation. Cancer biology & therapy *2*, 702-706.

Jensen, C.J., Buch, M.B., Krag, T.O., Hemmings, B.A., Gammeltoft, S., and Frodin, M. (1999). 90-kDa ribosomal S6 kinase is phosphorylated and activated by 3-phosphoinositide-dependent protein kinase-1. The Journal of biological chemistry *274*, 27168-27176.

Jeong, W.J., Yoon, J., Park, J.C., Lee, S.H., Lee, S.H., Kaduwal, S., Kim, H., Yoon, J.B., and Choi, K.Y. (2012). Ras stabilization through aberrant activation of Wnt/beta-catenin signaling promotes intestinal tumorigenesis. Science signaling *5*, ra30.

Johnson, L.R., Robinson, J.D., Lester, K.N., and Pitcher, J.A. (2013). Distinct structural features of G protein-coupled receptor kinase 5 (GRK5) regulate its nuclear localization and DNA-binding ability. PloS one *8*, e62508.

Ki, H., Oh, M., Chung, S.W., and Kim, K. (2008). Beta-catenin can bind directly to CRM1 independently of adenomatous polyposis coli, which affects its nuclear localization and LEF-1/beta-catenin-dependent gene expression. Cell biology international *32*, 394-400.
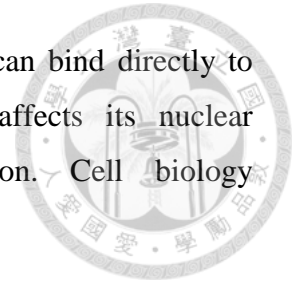
Kim, J., Parrish, A.B., Kurokawa, M., Matsuura, K., Freel, C.D., Andersen, J.L., Johnson, C.E., and Kornbluth, S. (2012). Rsk-mediated phosphorylation and 14-3-3varepsilon binding of Apaf-1 suppresses cytochrome c-induced apoptosis. The EMBO journal *31*, 1279-1292.

Kreimann, E.L., Morales, F.C., de Orbeta-Cruz, J., Takahashi, Y., Adams, H., Liu, T.J., McCrea, P.D., and Georgescu, M.M. (2007). Cortical stabilization of beta-catenin contributes to NHERF1/EBP50 tumor suppressor function. Oncogene *26*, 5290-5299.

Kufe, D., Inghirami, G., Abe, M., Hayes, D., Justi-Wheeler, H., and Schlom, J. (1984). Differential reactivity of a novel monoclonal antibody (DF3) with human malignant versus benign breast tumors. Hybridoma *3*, 223-232.

la Cour, T., Gupta, R., Rapacki, K., Skriver, K., Poulsen, F.M., and Brunak, S. (2003). NESbase version 1.0: a database of nuclear export signals. Nucleic acids research *31*, 393-396.

Lara, R., Seckl, M.J., and Pardo, O.E. (2013). The p90 RSK family members: common functions and isoform specificity. Cancer research *73*, 5301-5308.

Lecce, L., Lindsay, L.A., and Murphy, C.R. (2011). Ezrin and EBP50 redistribute apically in rat uterine epithelial cells at the time of implantation and in response to cell contact. Cell and tissue research *343*, 445-453.

Leighton, I.A., Dalby, K.N., Caudwell, F.B., Cohen, P.T., and Cohen, P. (1995). Comparison of the specificities of p70 S6 kinase and MAPKAP kinase-1 identifies a relatively specific substrate for p70 S6 kinase: the N-terminal kinase domain of MAPKAP kinase-1 is essential for peptide phosphorylation. FEBS letters *375*, 289-293.

Lin, Y.Y., Hsu, Y.H., Huang, H.Y., Shann, Y.J., Huang, C.Y., Wei, S.C., Chen, C.L., and Jou, T.S. (2012). Aberrant nuclear localization of EBP50 promotes colorectal carcinogenesis in xenotransplanted mice by modulating TCF-1 and beta-catenin interactions. The Journal of clinical investigation *122*, 1881-1894.

Liu, J.L., Yang, H.W., Chen, Z.S., and Jiang, Y. (2011). [Abnormal expression of RSK-4 and its clinical significance in breast cancer]. Zhonghua zhong liu za zhi [Chinese journal of oncology] *33*, 452-456.

Lo, H.W., Ali-Seyed, M., Wu, Y., Bartholomeusz, G., Hsu, S.C., and Hung, M.C. (2006). Nuclear-cytoplasmic transport of EGFR involves receptor endocytosis, importin beta1 and CRM1. Journal of cellular biochemistry *98*, 1570-1583.

Lu, K.P., Hanes, S.D., and Hunter, T. (1996). A human peptidyl-prolyl isomerase essential for regulation of mitosis. Nature *380*, 544-547.

Malfettone, A., Silvestris, N., Paradiso, A., Mattioli, E., Simone, G., and Mangia, A. (2012). Overexpression of nuclear NHERF1 in advanced colorectal cancer: association with hypoxic microenvironment and tumor invasive phenotype. Experimental and molecular pathology *92*, 296-303.

Mangia, A., Saponaro, C., Malfettone, A., Bisceglie, D., Bellizzi, A., Asselti, M., Popescu, O., Reshkin, S.J., Paradiso, A., and Simone, G. (2012). Involvement of nuclear NHERF1 in colorectal cancer progression. Oncology reports *28*, 889-894.

Mohler, P.J., Kreda, S.M., Boucher, R.C., Sudol, M., Stutts, M.J., and Milgram, S.L. (1999). Yes-associated protein 65 localizes p62(c-Yes) to the apical compartment of airway epithelia by association with EBP50. The Journal of cell biology *147*, 879-890.

Molina, J.R., Agarwal, N.K., Morales, F.C., Hayashi, Y., Aldape, K.D., Cote, G., and Georgescu, M.M. (2012). PTEN, NHERF1 and PHLPP form a tumor suppressor network that is disabled in glioblastoma. Oncogene *31*, 1264-1274.

Ossareh-Nazari, B., Bachelerie, F., and Dargemont, C. (1997). Evidence for a role of CRM1 in signal-mediated nuclear protein export. Science *278*, 141-144.

Paoli, P., Giannoni, E., and Chiarugi, P. (2013). Anoikis molecular pathways and its role in cancer progression. Biochimica et biophysica acta *1833*, 3481-3498.

Paradiso, A., Scarpi, E., Malfettone, A., Addati, T., Giotta, F., Simone, G., Amadori, D., and Mangia, A. (2013). Nuclear NHERF1 expression as a prognostic marker in breast cancer. Cell death & disease *4*, e904.

Pearson, H.B., Phesse, T.J., and Clarke, A.R. (2009). K-ras and Wnt signaling synergize to accelerate prostate tumorigenesis in the mouse. Cancer research *69*, 94-101.

Popa, I., Harris, M.E., Donello, J.E., and Hope, T.J. (2002). CRM1-dependent function of a cis-acting RNA export element. Molecular and cellular biology *22*, 2057-2067.

Raices, M., and D'Angelo, M.A. (2012). Nuclear pore complex composition: a new regulator of tissue-specific and developmental functions. Nature reviews Molecular cell biology *13*, 687-699.

Rapoport, T.A. (2007). Protein translocation across the eukaryotic endoplasmic reticulum and bacterial plasma membranes. Nature *450*, 663-669.

Reczek, D., Berryman, M., and Bretscher, A. (1997). Identification of EBP50: A PDZ-containing phosphoprotein that associates with members of the ezrin-radixin-moesin family. The Journal of cell biology *139*, 169-179.

Reczek, D., and Bretscher, A. (1998). The carboxyl-terminal region of EBP50 binds to a site in the amino-terminal domain of ezrin that is masked in the dormant molecule. The Journal of biological chemistry *273*, 18452-18458.

Richards, S.A., Dreisbach, V.C., Murphy, L.O., and Blenis, J. (2001). Characterization of regulatory events associated with membrane targeting of p90 ribosomal S6 kinase 1. Molecular and cellular biology *21*, 7470-7480.
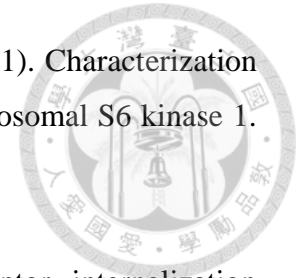
Rochdi, M.D., and Parent, J.L. (2003). Galphaq-coupled receptor internalization specifically induced by Galphaq signaling. Regulation by EBP50. The Journal of biological chemistry *278*, 17827-17837.

Romeo, Y., and Roux, P.P. (2011). Paving the way for targeting RSK in cancer. Expert opinion on therapeutic targets *15*, 5-9.

Romeo, Y., Zhang, X., and Roux, P.P. (2012). Regulation and function of the RSK family of protein kinases. The Biochemical journal *441*, 553-569.

Roux, P.P., Richards, S.A., and Blenis, J. (2003). Phosphorylation of p90 ribosomal S6 kinase (RSK) regulates extracellular signal-regulated kinase docking and RSK activity. Molecular and cellular biology *23*, 4796-4804.

Saha, M., Carriere, A., Cheerathodi, M., Zhang, X., Lavoie, G., Rush, J., Roux, P.P., and Ballif, B.A. (2012). RSK phosphorylates SOS1 creating 14-3-3-docking sites and negatively regulating MAPK activation. The Biochemical journal *447*, 159-166.

Schmidt, O., Pfanner, N., and Meisinger, C. (2010). Mitochondrial protein import: from proteomics to functional mechanisms. Nature reviews Molecular cell biology *11*, 655-667.

Scholz, R.P., Regner, J., Theil, A., Erlmann, P., Holeiter, G., Jahne, R., Schmid, S., Hausser, A., and Olayioye, M.A. (2009). DLC1 interacts with 14-3-3 proteins to inhibit RhoGAP activity and block nucleocytoplasmic shuttling. Journal of cell science *122*, 92-102.

Seimiya, H., Sawada, H., Muramatsu, Y., Shimizu, M., Ohko, K., Yamane, K., and Tsuruo, T. (2000). Involvement of 14-3-3 proteins in nuclear localization of telomerase. The EMBO journal *19*, 2652-2661.
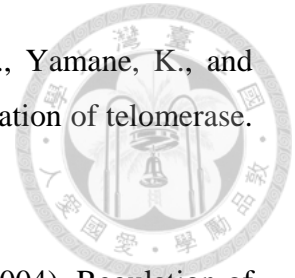
Shenolikar, S., Voltz, J.W., Cunningham, R., and Weinman, E.J. (2004). Regulation of ion transport by the NHERF family of PDZ proteins. Physiology *19*, 362-369.

Shibata, T., Chuma, M., Kokubu, A., Sakamoto, M., and Hirohashi, S. (2003). EBP50, a beta-catenin-associating protein, enhances Wnt signaling and is over-expressed in hepatocellular carcinoma. Hepatology *38*, 178-186.

Sneddon, W.B., Syme, C.A., Bisello, A., Magyar, C.E., Rochdi, M.D., Parent, J.L., Weinman, E.J., Abou-Samra, A.B., and Friedman, P.A. (2003). Activation-independent parathyroid hormone receptor internalization is regulated by NHERF1 (EBP50). The Journal of biological chemistry *278*, 43787-43796.

Sun, C., Zheng, J., Cheng, S., Feng, D., and He, J. (2013). EBP50 phosphorylation by Cdc2/Cyclin B kinase affects actin cytoskeleton reorganization and regulates functions of human breast cancer cell line MDA-MB-231. Molecules and cells *36*, 47-54.

Takenaka, Y., Fukumori, T., Yoshii, T., Oka, N., Inohara, H., Kim, H.R., Bresalier, R.S., and Raz, A. (2004). Nuclear export of phosphorylated galectin-3 regulates its antiapoptotic activity in response to chemotherapeutic drugs. Molecular and cellular biology *24*, 4395-4406.

Terry, L.J., Shows, E.B., and Wente, S.R. (2007). Crossing the nuclear envelope: hierarchical regulation of nucleocytoplasmic transport. Science *318*, 1412-1416.

Turner, J.G., Dawson, J., and Sullivan, D.M. (2012). Nuclear export of proteins and drug resistance in cancer. Biochemical pharmacology *83*, 1021-1032.

Wang, C., Zhao, R., Huang, P., Yang, F., Quan, Z., Xu, N., and Xi, R. (2013). APC loss-induced intestinal tumorigenesis in Drosophila: Roles of Ras in Wnt signaling activation and tumor progression. Developmental biology *378*, 122-140.

Wang, S., Raab, R.W., Schatz, P.J., Guggino, W.B., and Li, M. (1998). Peptide binding consensus of the NHE-RF-PDZ1 domain matches the C-terminal sequence of cystic fibrosis transmembrane conductance regulator (CFTR). FEBS letters *427*, 103-108.

Weinman, E.J., Minkoff, C., and Shenolikar, S. (2000). Signal complex regulation of renal transport proteins: NHERF and regulation of NHE3 by PKA. American journal of physiology Renal physiology *279*, F393-399.

Weinman, E.J., Steplock, D., Wang, Y., and Shenolikar, S. (1995). Characterization of a protein cofactor that mediates protein kinase A regulation of the renal brush border membrane Na(+)-H+ exchanger. The Journal of clinical investigation *95*, 2143-2149.

Weinman, E.J., Wang, Y., Wang, F., Greer, C., Steplock, D., and Shenolikar, S. (2003). A C-terminal PDZ motif in NHE3 binds NHERF-1 and enhances cAMP inhibition of sodium-hydrogen exchange. Biochemistry *42*, 12662-12668.

Wen, Y., Caffrey, T.C., Wheelock, M.J., Johnson, K.R., and Hollingsworth, M.A. (2003). Nuclear association of the cytoplasmic tail of MUC1 and beta-catenin. The Journal of biological chemistry *278*, 38029-38039.

Wente, S.R., and Rout, M.P. (2010). The nuclear pore complex and nuclear transport. Cold Spring Harbor perspectives in biology *2*, a000562.

Wickner, W., and Schekman, R. (2005). Protein translocation across biological membranes. Science *310*, 1452-1456.

Wolff, B., Sanglier, J.J., and Wang, Y. (1997). Leptomycin B is an inhibitor of nuclear export: inhibition of nucleo-cytoplasmic translocation of the human immunodeficiency virus type 1 (HIV-1) Rev protein and Rev-dependent mRNA. Chemistry & biology *4*, 139-147.

Wu, J., and Janknecht, R. (2002). Regulation of the ETS transcription factor ER81 by the 90-kDa ribosomal S6 kinase 1 and protein kinase A. The Journal of biological chemistry *277*, 42669-42679.

Xu, W., Wang, Z., Zhang, W., Qian, K., Li, H., Kong, D., Li, Y., and Tang, Y. (2015). Mutated K-ras activates CDK8 to stimulate the epithelial-to-mesenchymal transition in pancreatic cancer in part via the Wnt/beta-catenin signaling pathway. Cancer letters *356*, 613-627.

Yaffe, M.B., Rittinger, K., Volinia, S., Caron, P.R., Aitken, A., Leffers, H., Gamblin, S.J., Smerdon, S.J., and Cantley, L.C. (1997). The structural basis for 14-3-3:phosphopeptide binding specificity. Cell *91*, 961-971.

Yang, X., Lee, W.H., Sobott, F., Papagrigoriou, E., Robinson, C.V., Grossmann, J.G., Sundstrom, M., Doyle, D.A., and Elkins, J.M. (2006). Structural basis for protein-protein interactions in the 14-3-3 protein family. Proc Natl Acad Sci U S A *103*, 17237-17242.

Zhang, X., Lavoie, G., Fort, L., Huttlin, E.L., Tcherkezian, J., Galan, J.A., Gu, H., Gygi, S.P., Carreno, S., and Roux, P.P. (2013). Gab2 phosphorylation by RSK inhibits Shp2 recruitment and cell motility. Molecular and cellular biology *33*, 1657-1670.

Zhao, Y., Bjorbaek, C., and Moller, D.E. (1996). Regulation and interaction of pp90(rsk) isoforms with mitogen-activated protein kinases. The Journal of biological chemistry *271*, 29773-29779.

Zhu, J., Blenis, J., and Yuan, J. (2008). Activation of PI3K/Akt and MAPK pathways regulates Myc-mediated transcription by phosphorylating and promoting the degradation of Mad1. Proceedings of the National Academy of Sciences of the United States of America *105*, 6584-6589.
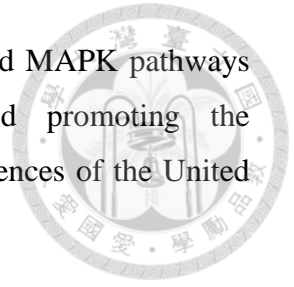
Appendix I   **Genes analysed in RNAi screen and the EGFP-EBP50 nuclear localization scores**

Kinase and Phosphatase		No. of shRNA					
		EGFP N-C (shGene/shVC)					
Gene Symbol	Acession No.	≥2.00	1.50-1.99	1.00-1.49	0.51-0.99	0.5-0.11	≤ 0.10
AAK1	NM_014911			2	3		
AATK	XM_375495				4		
ABL2	NM_005158		1	2	2		
ACACA	NM_000664			3	2		
ACACB	NM_001093				4		
ACVR1B	NM_004302			5			
ACVR1C	NM_145259			5			
ACVRL1	NM_000020			4			
ADCK1	NM_020421			2	3		
ADCK2	NM_052853			1	4		
ADCK4	NM_024876			1	4		
ADCK5	NM_174922			3	1		
ADRBK2	NM_005160			3	1		
AGTR2	NM_000686			1	3		
AK1	NM_000476			1	3		
AK2	NM_001625			1	4		
AK3	NM_016282			1	4		
AK5	NM_012093			1	4		
AKAP11	NM_016248			3	2		
AKAP5	NM_004857				4		
AKT2	NM_001626			1	3		
AKT3	NM_005465			4	1		
ALK	NM_004304			5			
ALPK1	NM_025144			3	2		
ALPK2	NM_052947			1	4		
ALPK3	NM_020778				4		
ALS2CR7	NM_139158			3	2		
AMFR	NM_001144				3		
AMHR2	NM_020547			2	3		
ANKK1	NM_178510			1	2		
APEG1	NM_005876				5		
APOB	NM_000384			2	3		
APPL	NM_012096			3	1		
ARHGAP29	NM_004815			2	3		
ARHGEF2	NM_004723			1	3		
ATM	NM_000051			3	2		
ATXN1	NM_000332			1	4		
AURKB	NM_004217		1	3			
AURKC	NM_001015878			3	1		
AXL	NM_021913			2	3		
BARD1	NM_000465				5		
BCL2L11	NM_138621			2	2		
BCR	NM_004327			1	4		
BIRC2	NM_001166				5		
BIRC3	NM_001165				5		
BIRC4	NM_001167			1	3		
BMP2K	NM_017593			1	4		
BMPR1A	NM_004329			1	3	1	

Kinase and Phosphatase		No. of shRNA					
		EGFP N-C (shGene/shVC)					
Gene Symbol	Acession No.	≥2.00	1.50-1.99	1.00-1.49	0.51-0.99	0.5-0.11	≤ 0.10
BMX	NM_001721				4		
BRAF	NM_004333				5		
BRCA2	NM_000059		1	4			
BRD2	NM_005104			2	3		
BRD3	NM_007371			2	3		
BRD4	NM_058243		3	2			
BRDT	NM_001726			1	4		
BRSK1	NM_032430			4	1		
BRSK2	NM_003957			5			
BTK	NM_000061			3	2		
BUB1	NM_004336			4			
C17orf31	NM_017575			4	1		
C17orf51	XM_378661			3	1		
C7orf16	NM_006658			4	1		
CABC1	NM_020247				5		
CAMK1	NM_003656		1	4			
CAMK1D	NM_153498			4			
CAMK1G	NM_020439			4	1		
CAMKK1	NM_172207			4	1		
CAMKK2	NM_153499			2	3		
CASK	NM_003688			3	2		
CBL	NM_005188			5			
CBLB	NM_170662				4		
CCL2	NM_002982			2	3		
CCR2	NM_000648			3	2		
CCRK	NM_178432			2	2		
CCRN4L	NM_012118			4	1		
CDC14A	NM_003672			2	3		
CDC14B	NM_003671				3		
CDC14C	NM_152627				5		
CDC20	NM_001255				5		
CDC25A	NM_001789			1	2		
CDC25B	NM_004358			2	3		
CDC25C	NM_001790			2	2		
CDC2L1	NM_001787			2	3		
CDC2L2	NM_024011				5		
CDC2L5	NM_003718			5			
CDC2L6	NM_015076			4	1		
CDC42BPA	NM_003607			2	2		
CDC42BPB	NM_006035			4			
CDC42BPG	XM_290516			1	3		
CDC7	NM_003503				5		
CDH1	NM_004360		1	3	1		
CDK10	NM_003674			3	2		
CDK2	NM_001798			1	4		
CDK4	NM_000075			4			
CDK5	NM_004935			1	4		
CDK5R1	NM_003885			1	4		

Kinase and Phosphatase		No. of shRNA					
		EGFP N-C (shGene/shVC)					
Gene Symbol	Acession No.	≥2.00	1.50-1.99	1.00-1.49	0.51-0.99	0.5-0.11	≤ 0.10
CDK6	NM_001145306			5			
CDKL1	NM_004196			2	3		
CDKL2	NM_003948		1	3	1		
CDKL3	NM_001113575			5			
CDKL4	XM_293029			1	4		
CDKL5	NM_003159		1	1	3		
CDKN1A	NM_000389			3	2		
CDKN1C	NM_000076			4	1		
CDKN2A	NM_000077			4			
CDKN3	NM_005192			1	4		
CHEK2	NM_001005735			4	1		
CHKA	NM_001277				5		
CILP	NM_003613			3	2		
CIT	NM_007174			2	3		
CKB	NM_001823				4		
CKMT1B	NM_020990				5		
CKMT2	NM_001825				4		
CLK1	NM_004071		3	1	1		
CLK2	NM_003993			4			
CLK3	NM_003992		1	2	2		
CMPK	NM_016308			4	1		
COL3A1	NM_000090			2	3		
COL4A3BP	NM_005713			1	4		
CPNE1	NM_152928			3	1		
CPNE2	NM_152727			1	4		
CPNE3	NM_003909			5			
CPT2	NM_000098			1	4		
CRK7	NM_016507			1	4		
CRKL	NM_005207				5		
CSF1R	NM_005211			1	2		
CSK	NM_004383			3	2		
CSNK1A1	NM_001892				4		
CSNK1A1L	NM_145203			2	3		
CSNK1E	NM_152221			4	1		
CSNK1G3	NM_004384			4			
CSNK2A1	NM_001895		1	3	1		
CSNK2A2	NM_001896			3	2		
CSNK2B	NM_001320			1	3		
CTDP1	NM_004715			2	2		
CTDSP2	NM_005730			3			
CTDSPL	NM_005808			5			
CXCL12	NM_000609				5		
DAB2IP	NM_032552		1	3	1		
DAPK1	NM_004938			3	1		
DAPK2	NM_014326			4	1		
DAXX	NM_001350			3	2		
DCAMKL1	NM_004734			5			
DCAMKL3	NM_033403			2	3		

Appendix I (*cont'd 3*)   Genes analysed in RNAi screen and the EGFP-EBP50 nuclear localization scores

Kinase and Phosphatase		No. of shRNA					
		EGFP N-C (shGene/shVC)					
Gene Symbol	Acession No.	≥2.00	1.50-1.99	1.00-1.49	0.51-0.99	0.5-0.11	≤ 0.10
DCLK2	NM_152619			1	4		
DDR1	NM_001954			3	1		
DDR2	NM_006182		1	4			
DDX5	NM_004396		2	3			
DGKA	NM_001345			1	4		
DGKB	NM_004080			5			
DGKD	NM_003648			4	1		
DGKE	NM_003647				5		
DGKI	NM_004717				4		
DGKQ	NM_001347				4		
DGUOK	NM_001929			2	2		
DHX16	NM_003587			5			
DKC1	NM_001142463			5			
DKFZp761P0423	XM_291277				5		
DLG1	NM_004087				5		
DLG2	NM_001364				5		
DLG4	NM_001365				5		
DMPK	NM_004409			5			
DNAJC6	NM_014787			2	2		
DNM1L	NM_012062		1	2			
DOCK2	NM_004946		1	1	3		
DOCK4	NM_014705			4	1		
DTYMK	NM_012145				4		
DULLARD	NM_015343			3	2		
DUSP1	NM_004417			3	2		
DUSP10	NM_007207			3	2		
DUSP11	NM_003584			1	4		
DUSP12	NM_007240			3	1		
DUSP13	NM_016364			1	4		
DUSP14	NM_007026			5			
DUSP15	NM_080611			2	3		
DUSP18	NM_152511			2	3		
DUSP19	NM_080876			3	2		
DUSP21	NM_022076			2	3		
DUSP22	NM_020185			4	1		
DUSP3	NM_004090			3	2		
DUSP4	NM_001394			2	2		
DUSP5	NM_004419			3	1		
DUSP6	NM_001946			1	2		
DUSP9	NM_001395			1	2		
DYRK1B	NM_004714		1	2	2		
DYRK2	NM_003583			2	3		
DYRK3	NM_001004023			4			
DYRK4	NM_003845			3	1		
DYSF	NM_003494			4	1		
EEF2K	NM_013302			1	4		
EGLN1	NM_022051			2	2		
EGLN3	NM_022073			4	1		

Appendix I (*cont'd 4*)   **Genes analysed in RNAi screen and the EGFP-EBP50 nuclear localization scores**

Kinase and Phosphatase		No. of shRNA					
		EGFP N-C (shGene/shVC)					
Gene Symbol	Acession No.	≥2.00	1.50-1.99	1.00-1.49	0.51-0.99	0.5-0.11	≤ 0.10
ENPP1	NM_006208			2	3		
ENPP6	NM_153343				4		
ENPP7	NM_178543			3	1		
EPHA1	NM_005232				5		
EPHA10	NM_173641			2	2		
EPHA2	NM_004431			1	4		
EPHA3	NM_005233				4		
EPHA5	NM_004439			2	3		
EPHA6	XM_496653			3	1		
EPHB1	NM_004441		3	2			
EPHB2	NM_004442			2	2		
EPHB3	NM_004443			1	3		
EPHB4	NM_004444			4	1		
EPHB6	NM_004445			2	1		
ERBB3	NM_001982			2	2		
ERBB4	NM_005235			5			
ERCC8	NM_000082			4	1		
ESR1	NM_000125			1	3		
ESR2	NM_001437				4		
EVI1	NM_005241			2	3		
EXOSC10	NM_002685			1	3		
EXT1	NM_000127			1	4		
EZH1	NM_001991			1	3		
FAM62A	NM_015292			5			
FASN	NM_004104			4	1		
FASTK	NM_006712			2	3		
FER	NM_005246			5			
FES	NM_001143783			3	1		
FGF2	NM_002006				5		
FGFR1	NM_015850			3	2		
FGFR2	NM_000141			4	1		
FGFR3	NM_000142			3	1		
FGFR4	NM_002011			3			
FGR	NM_005248			2	3		
FKBP8	NM_012181		3	1			
FLJ25006	NM_144610			1	3		
FLJ40125	NM_178494			1	2		
FLJ40852	NM_173677				5		
FLT1	NM_001159920			5			
FLT3	NM_004119			3	1		
FLT4	NM_002020			3	2		
FSHR	NM_000145			1	4		
FUS	NM_004960			5			
FXN	NM_000144			1	3		
FYN	NM_002037			1	4		
GAK	NM_005255			1	4		
GEFT	NM_001111270			3	2		
GGT7	NM_178026			4	1		

Kinase and Phosphatase		No. of shRNA					
		EGFP N-C (shGene/shVC)					
Gene Symbol	**Acession No.**	**≥2.00**	**1.50-1.99**	**1.00-1.49**	**0.51-0.99**	**0.5-0.11**	**≤ 0.10**
GMFB	NM_004124			4	1		
GMFG	NM_004877			3	1		
GMIP	NM_016573			2	2		
GNE	NM_005476			3	2		
GPR109a	NM_030701			1	4		
GPR119	XM_066873			2	3		
Gpr12	NM_008151			2	3		
GRK1	NM_002929			1	3		
GRK4	NM_005307			3	2		
GRK5	NM_005308			2	2		
GRK7	NM_139209			2	2		
GSC	NM_173849			4	1		
GSG2	NM_031965				5		
GSK3B	NM_002093		1	3	1		
GTF2H1	NM_005316			2	3		
GUCY2C	NM_004963			1	4		
GUCY2D	NM_000180			3	1		
GUK1	NM_000858				5		
HIPK1	NM_152696			1	4		
HIPK2	NM_022740			1	3		
HIPK3	NM_005734			1	4		
HIPK4	NM_144685				5		
HNRPA2B1	NM_002137			3			
HRAS	NM_176795			1	4		
HSPA5	NM_005347				3		
HSPCA	NM_005348			2	3		
HUNK	NM_014586			1	4		
HYPB	NM_012271			3	2		
ICK	NM_014920			2	3		
IGBP1	NM_001551			3	2		
IGF1R	NM_000875			5			
IHPK2	NM_016291			1	4		
IKBKB	NM_001556			3	2		
ILK	NM_004517		1	4			
ILKAP	NM_030768		1	2	2		
ILVBL	NM_176826				4		
INPP4A	NM_004027			3	2		
INSR	NM_000208			3	2		
INSRR	NM_014215			1	3		
IRAK3	NM_007199			5			
IRAK4	NM_016123			4			
ITCH	NM_031483			3	1		
ITGAV	NM_002210			2	1		
ITGB3	NM_000212			2	3		
ITSN1	NM_003024			2	2		
ITSN2	NM_006277			3	2		
JAK1	NM_002227			1	3		
JAK2	NM_004972			1	4		

Kinase and Phosphatase		No. of shRNA					
		EGFP N-C (shGene/shVC)					
Gene Symbol	Acession No.	≥2.00	1.50-1.99	1.00-1.49	0.51-0.99	0.5-0.11	≤ 0.10
JAK3	NM_000215			4	1		
JMJD7-PLA2G4B	NM_005090			2	1		
KDR	NM_002253			3	2		
KIAA0226	XM_032901			1	3		
KIAA0999	NM_025164				4		
KIAA1706	NM_030636			3	1		
KIAA1804	NM_032435			2	3		
KIAA2002	XM_370878				5		
KIT	NM_000222			4	1		
KLHL23	NM_144711				5		
KRAS	NM_004985			3	2		
KSR	XM_290793				5		
KSR2	NM_173598			3	2		
LATS1	NM_004690			3	2		
LATS2	NM_014572		1	4			
LCK	NM_005356			1	4		
LIG4	NM_001098268			4	1		
LMTK3	XM_055866			3	2		
LOC151649	NM_144714			3	2		
LOC390975	XM_372749				4		
LRPPRC	NM_133259				5		
LRRK1	NM_024652			3	2		
LRRK2	XM_058513			1	4		
LTK	NM_002344			2	2		
MAK	NM_005906			3	1		
MAMDC2	NM_153267				5		
MAML1	NM_014757				5		
MAP2K1	NM_002755			4	1		
MAP2K2	NM_030662			1	3		
MAP2K5	NM_145162			4	1		
MAP3K1	XM_042066			3	2		
MAP3K10	NM_002446			2	2		
MAP3K11	NM_002419			2	3		
MAP3K12	NM_006301			3	2		
MAP3K13	NM_004721			3	2		
MAP3K14	NM_003954			3	1		
MAP3K15	XM_372199				5		
MAP3K2	NM_006609			2	3		
MAP3K3	NM_002401		1	1	2		
MAP3K4	NM_005922			2	2		
MAP3K5	NM_005923			2	3		
MAP3K6	NM_004672			3	1		
MAP3K7IP1	NM_006116			4	1		
MAP3K9	XM_027237			1	4		
MAP4K1	NM_007181			3	2		
MAP4K2	NM_004579			2	3		
MAP4K3	NM_003618			3	1		
MAP4K4	NM_145687		1	2	2		

Kinase and Phosphatase		No. of shRNA					
		EGFP N-C (shGene/shVC)					
Gene Symbol	Acession No.	≥2.00	1.50-1.99	1.00-1.49	0.51-0.99	0.5-0.11	≤ 0.10
MAP4K5	NM_006575			1	4		
MAPK10	NM_002753			4	1		
MAPK12	NM_002969				5		
MAPK13	NM_002754			3	1		
MAPK15	NM_139021			1	2		
MAPK3	NM_002746			1	2		
MAPK6	NM_002748			3	1		
MAPK8	NM_005456		1	2			
MAPK9	NM_139069			4	1		
MAPKAP1	NM_024117			3	1		
MAPKAPK2	NM_032960				5		
MAPKAPK3	NM_004635			2	3		
MAPKAPK5	NM_003668			3	1		
MARK1	NM_018650			3	2		
MARK2	NM_004954			3	2		
MARK3	NM_002376			3	1		
MARK4	NM_031417				5		
MAST1	NM_014975			2	1		
MAST2	NM_015112			3			
MAST3	XM_038150				5		
MAST4	XM_291141			1	4		
MASTL	NM_032844			2	3		
MATK	NM_002378			2	3		
MBIP	NM_016586				5		
MCTP1	NM_024717			2	3		
MCTP2	NM_018349			3	2		
MDGA2	NM_182830				5		
MDM2	NM_002392			3	2		
MELK	NM_014791			3	2		
MEN1	NM_000244			1	4		
MERTK	NM_006343		1	3	1		
MET	NM_000245			3	2		
MINK1	NM_015716				3		
MKNK1	NM_003684				4		
MKNK2	NM_017572			1	4		
MLCK	NM_182493			5			
MLKL	NM_152649			2	3		
MLLT7	NM_005938			5			
MMP1	NM_002421				5		
MMP3	NM_002422			1	3		
MORC1	NM_014429			2	3		
MOS	NM_005372			2	1		
MPP1	NM_002436			1	4		
MPP2	NM_005374			2	3		
MPP3	NM_001932			2	3		
MSH2	NM_000251		1	4			
MSH5	NM_002441			2	3		
MST1R	NM_002447			1	4		

Kinase and Phosphatase		No. of shRNA					
		EGFP N-C (shGene/shVC)					
Gene Symbol	Acession No.	≥2.00	1.50-1.99	1.00-1.49	0.51-0.99	0.5-0.11	≤ 0.10
MTM1	NM_000252			1	3		
MTMR1	NM_003828			2	3		
MTMR2	NM_016156			2	3		
MTMR3	NM_021090			3	2		
MTMR4	NM_004687			2	3		
MTMR6	NM_004685			3	1		
MUSK	NM_005592			1	3		
MYLK	NM_053028			3			
MYLK2	NM_033118			3			
MYO3A	NM_017433				5		
MYO3B	NM_001083615			5			
MYO9B	NM_004145			3	2		
MYST2	NM_007067		1	1	3		
NBN	NM_002485			5			
NEDD4L	NM_015277			4	1		
NEK1	NM_012224			2	3		
NEK10	NM_152534			2	3		
NEK11	NM_024800			4	1		
NEK2	NM_002497			5			
NEK3	NM_152720			2	3		
NEK4	NM_003157			2	3		
NEK5	XM_292160			2	3		
NEK6	NM_014397			4	1		
NEK7	NM_133494			4			
NEK8	NM_178170			3	2		
NEK9	NM_033116			4			
NF1	NM_000267			5			
NF2	NM_000268			2	3		
NKX3-1	NM_006167			3	1		
NLK	NM_016231			1	4		
NME5	NM_003551			1	4		
NOS2A	NM_000625				5		
NOTCH1	NM_017617			1	4		
NOVA1	NM_006491		1	3			
NPR1	NM_000906			1	4		
NPR2	NM_003995		1	3			
NQO1	NM_000903				5		
NR1H4	NM_005123			3	2		
NR1I2	NM_003889			3	2		
NR1I3	NM_001077469			4	1		
NRBP	NM_013392		1	3	1		
NRBP2	NM_178564				5		
NTRK1	NM_002529			2	3		
NTRK2	NM_006180			2	3		
NTRK3	NM_002530			2	3		
NUAK1	NM_014840		1	3	1		
NUAK2	NM_030952			3	1		
OBSCN	NM_052843			5			

Kinase and Phosphatase		No. of shRNA					
		EGFP N-C (shGene/shVC)					
Gene Symbol	Acession No.	≥2.00	1.50-1.99	1.00-1.49	0.51-0.99	0.5-0.11	≤ 0.10
OTOF	NM_194323			1	4		
OXSR1	NM_005109				4		
PAK1	NM_002576			1	3		
PAK2	NM_002577				5		
PAK3	NM_002578				5		
PAK6	NM_020168			3			
PAK7	NM_020341			2	3		
PASK	NM_015148			1	3		
PBK	NM_018492			4	1		
PCTK2	NM_002595			1	4		
PCTK3	NM_002596			3	2		
PDGFRA	NM_006206		1	3	1		
PDGFRB	NM_002609			2	3		
PDIK1L	NM_152835			2	3		
PDK1	NM_002610			1	3		
PDK2	NM_002611				5		
PDK4	NM_002612			4	1		
PDPK1	NM_002613			3	2		
PFTK1	NM_012395			4			
PGK1	NM_000291				5		
PGR	NM_000926				4		
PHKG1	NM_006213				5		
PHKG2	NM_000294			4	1		
PHOSPHO1	NM_178500				4		
PIK3C2A	NM_002645			2	3		
PIK3C2B	NM_002646			2	3		
PIK3C2G	NM_004570			5			
PIK3CB	NM_006219			1	3		
PIK3R2	NM_005027			5			
PIK3R4	NM_014602			4			
PIM2	NM_006875			3	2		
PIM3	NM_001001852				3		
PIN1	NM_006221			4			
PINK1	NM_032409			3	2		
PIP5K2A	NM_005028			1	3		
PIP5K2B	NM_003559			1	4		
PKIA	NM_006823			4	1		
PKIB	NM_032471			2	3		
PKLR	NM_000298			1	2		
PKMYT1	NM_004203			1	2		
PKN1	NM_002741			2	3		
PKN2	NM_006256				5		
PKN3	NM_013355			3	1		
PLCB1	NM_182734			1	3		
PLCB2	NM_004573			1	4		
PLCB4	NM_000933				5		
PLCD1	NM_001130964			2	2		
PLCD4	NM_032726			3	2		

Kinase and Phosphatase		No. of shRNA					
		EGFP N-C (shGene/shVC)					
Gene Symbol	Acession No.	≥2.00	1.50-1.99	1.00-1.49	0.51-0.99	0.5-0.11	≤ 0.10
PLCG1	NM_002660				4		
PLCG2	NM_002661			2	2		
PLCL2	NM_015184			4			
PLD1	NM_002662			3			
PLK1	NM_005030			1	3		
PLK2	NM_006622		1	3			
PLK3	NM_004073			5			
PLK4	NM_014264			3	2		
PMVK	NM_006556			1	3		
PNCK	NM_001039582			4	1		
PPARA	NM_005036			3	2		
PPARD	NM_006238			1	3		
PPARG	NM_011146			3	2		
PPEF1	NM_006240			3	2		
PPEF2	NM_006239			2	3		
PPFIA1	NM_003626			2	3		
PPFIA2	NM_003625			1	4		
PPFIA3	NM_003660			2	3		
PPFIBP1	NM_003622		1	1	3		
PPM1B	NM_002706			3	1		
PPM1D	NM_003620			5			
PPM1E	NM_014906			3	2		
PPM1F	NM_014634			2	1		
PPM1K	NM_152542			2	3		
PPM1L	NM_139245			1	4		
PPM1M	NM_144641			3	1		
PPM2C	NM_018444				5		
PPME1	NM_016147				4		
PPP1CA	NM_002708			2	3		
PPP1CB	NM_002709			3	2		
PPP1CC	NM_002710			5			
PPP1R11	NM_021959			2	2		
PPP1R12A	NM_002480			3	2		
PPP1R12B	NM_002481			3	2		
PPP1R12C	NM_017607			1	2		
PPP1R13B	NM_015316			3	2		
PPP1R14A	NM_033256				5		
PPP1R14C	NM_030949			3	2		
PPP1R14D	NM_017726			3	1		
PPP1R15A	NM_014330			2	3		
PPP1R15B	NM_032833			5			
PPP1R16A	NM_032902			4			
PPP1R16B	NM_015568			3	2		
PPP1R1A	NM_006741			1	4		
PPP1R3A	NM_002711			3	2		
PPP1R3C	NM_005398			2	2		
PPP1R7	NM_002712		1	4			
PPP1R9B	NM_032595			2	1		

Kinase and Phosphatase		No. of shRNA					
		EGFP N-C (shGene/shVC)					
Gene Symbol	Acession No.	≥2.00	1.50-1.99	1.00-1.49	0.51-0.99	0.5-0.11	≤ 0.10
PPP2CA	NM_002715			2	3		
PPP2CB	NM_004156			5			
PPP2R2A	NM_002717				5		
PPP2R2B	NM_001127381			5			
PPP2R2C	NM_020416			4	1		
PPP2R3A	NM_002718			2	3		
PPP2R3B	NM_013239			2	2		
PPP2R4	NM_178001			4			
PPP2R5B	NM_006244			4	1		
PPP2R5C	NM_002719		1	3	1		
PPP2R5D	NM_006245			2	2		
PPP2R5E	NM_006246			1	4		
PPP3CA	NM_000944			3	2		
PPP3CB	NM_001142353			5			
PPP3CC	NM_005605			3	2		
PPP3R1	NM_000945				5		
PPP3R2	NM_147180			2	3		
PPP4C	NM_002720			3	1		
PPP5C	NM_006247			3	2		
PPP6C	NM_002721			1	4		
PRKAA1	NM_006251			4	1		
PRKAA2	NM_006252			2	3		
PRKAB1	NM_006253			2	3		
PRKAB2	NM_005399			4	1		
PRKACB	NM_002731			4	1		
PRKACG	NM_002732			2	2		
PRKAG1	NM_002733			1	4		
PRKAG2	NM_016203			3	2		
PRKAG3	NM_017431				4		
PRKAR1A	NM_002734			4	1		
PRKCA	NM_002737			2	3		
PRKCB1	NM_002738				4		
PRKCE	NM_005400			5			
PRKCG	NM_002739			3	1		
PRKCH	NM_006255			2	3		
PRKCI	NM_002740			2	3		
PRKCQ	NM_006257			4	1		
PRKD1	NM_002742			3	2		
PRKD2	NM_016457			2	2		
PRKD3	NM_005813			4	1		
PRKDC	NM_006904			1	3		
PRKG1	NM_006258			3	1		
PRKX	NM_005044			3	1		
PRKY	NM_002760			3			
PRPF4B	NM_003913			5			
PRSS7	NM_002772			3	2		
PSKH1	NM_006742			4	1		
PSKH2	NM_033126			3	2		

Kinase and Phosphatase		No. of shRNA					
		EGFP N-C (shGene/shVC)					
Gene Symbol	Acession No.	≥2.00	1.50-1.99	1.00-1.49	0.51-0.99	0.5-0.11	≤ 0.10
PSPH	NM_004577			5			
PSTPIP1	NM_003978			1	3		
PSTPIP2	NM_024430			4	1		
PTBP2	NM_021190		1	4			
PTEN	NM_000314			2	3		
PTHR1	NM_000316			1	3		
PTK2	NM_005607			1	4		
PTK2B	NM_004103			3			
PTK6	NM_005975			2	2		
PTK7	NM_002821			2	3		
PTN	NM_002825			3			
PTP4A1	NM_003463			4	1		
PTP4A2	NM_003479			4			
PTPDC1	NM_152422			1	4		
PTPLA	NM_014241			3	2		
PTPN1	NM_002827			2	2		
PTPN11	NM_002834				5		
PTPN12	NM_001131008			3	2		
PTPN13	NM_006264			5			
PTPN14	NM_005401			3	2		
PTPN18	NM_014369			1	2		
PTPN2	NM_002828			2	3		
PTPN21	NM_007039			4	1		
PTPN22	NM_012411			2	3		
PTPN23	NM_015466				5		
PTPN3	NM_002829			3	1		
PTPN4	NM_002830			2	3		
PTPN5	NM_032781			4			
PTPN6	NM_002831			3	1		
PTPN7	NM_002832			5			
PTPN9	NM_002833			5			
PTPNS1	NM_080792			3	2		
PTPNS1L2	NM_178460			2	2		
PTPRA	NM_002836			4	1		
PTPRB	NM_001109754			4	1		
PTPRC	NM_002838			3	2		
PTPRD	NM_001040712			3	2		
PTPRE	NM_006504			2	2		
PTPRF	NM_002840			3	2		
PTPRG	NM_002841			5			
PTPRH	NM_001161440			2	2		
PTPRJ	NM_002843			4			
PTPRK	NM_001135648			5			
PTPRM	NM_002845		1	5	1		
PTPRN	NM_002846			5			
PTPRN2	NM_002847				5		
PTPRO	NM_002848			2	3		
PTPRR	NM_002849			1	3		

Appendix I (*cont'd 13*) Genes analysed in RNAi screen and the EGFP-EBP50 nuclear localization scores

Kinase and Phosphatase		No. of shRNA					
		EGFP N-C (shGene/shVC)					
Gene Symbol	Acession No.	≥2.00	1.50-1.99	1.00-1.49	0.51-0.99	0.5-0.11	≤ 0.10
PTPRS	NM_002850			2	3		
PTPRT	NM_007050			4			
PTPRU	NM_005704			3	1		
PTPRZ1	NM_002851			2	2		
PXK	NM_017771		1	4			
RAB11FIP5	NM_015470			3	1		
RAF1	NM_002880			5			
RAGE	NM_014226			5			
RASA2	NM_006506			2	3		
RASA3	NM_007368			2	3		
RASAL2	NM_004841			2	1		
RASSF5	NM_031437			2	3		
RB1	NM_000321			2	3		
RBL1	NM_002895			3	2		
REL	NM_002908			3	2		
RET	NM_020630			4	1		
RGS3	NM_134427			3	1		
RHO	NM_000539			1	4		
RIMS1	NM_014989			3	2		
RIMS2	NM_014677			5			
RIMS4	NM_182970			1	4		
RIOK1	NM_031480			1	3		
RIOK3	NM_003831			1	4		
RIPK1	NM_003804		1	4			
RIPK2	NM_003821			3	2		
RIPK3	NM_006871			1	4		
RIPK4	NM_020639				5		
RNASEL	NM_021133			5			
ROCK1	NM_005406				5		
ROCK2	NM_004850			3	2		
ROR1	NM_005012			2	3		
ROS1	NM_002944		1	3	1		
RP11-145H9.1	XM_373109			1	4		
RP6-213H19.1	NM_016542			2	3		
RPGRIP1	NM_020366			1	4		
RPS6KA1 (RSK1)	NM_002953			1	2	2	
RPS6KA2	NM_021135				4		
RPS6KA3	NM_004586				5		
RPS6KA4	NM_003942			2	2		
RPS6KA6	NM_014496				5		
RPS6KB1	NM_003161			3	2		
RPS6KC1	NM_012424			1	4		
RPS6KL1	NM_031464			2	3		
RSC1A1	NM_006511			3	2		
RXRA	NM_002957			3	2		
RXRB	NM_021976			4	1		
RXRG	NM_006917			3	2		
RYK	NM_002958			1	4		

Appendix I (*cont'd 14*) Genes analysed in RNAi screen and the EGFP-EBP50 nuclear localization scores

Kinase and Phosphatase		No. of shRNA					
		EGFP N-C (shGene/shVC)					
Gene Symbol	Acession No.	≥2.00	1.50-1.99	1.00-1.49	0.51-0.99	0.5-0.11	≤ 0.10
SAG	NM_000541			2	2		
SART1	NM_005146		1	3			
SBF1	NM_002972			3			
SBK1	XM_370948				4		
SCYL1	NM_020680			2	3		
SCYL2	NM_017988			2	3		
SCYL3	NM_020423		1	3			
SF1	NM_004630			5			
SFN	NM_006142		2	2	1		
SFPQ	NM_005066		1	2	1		
SFRS1	NM_006924	1		3			
SFRS7	NM_006276			5			
SGK	NM_001143676			3	2		
SGK2	NM_170693			1	3		
SKAP1	NM_003726			1	4		
SKI	NM_003036			5			
SLK	NM_014720			4	1		
SLU7	NM_006425		2	3			
SMG1	NM_014006			1	4		
SMNDC1	NM_005871			5			
SNCA	NM_000345				4		
SNRK	NM_017719			2	3		
SNW1	NM_012245			5			
SOCS5	NM_014011		1	4			
SRMS	NM_080823			4	1		
SRPK2	NM_003138			2	3		
SRPK3	NM_014370			1	2		
SSH1	NM_018984				4		
SSH2	NM_033389			1	4		
STAC3	NM_145064			1	3		
STK10	NM_005990			3	2		
STK11	NM_000455			5			
STK16	NM_001008910		1	3	1		
STK17A	NM_004760			3	1		
STK17B	NM_004226			3	1		
STK24	NM_001032296			5			
STK25	NM_006374			2	3		
STK3	NM_006281			3	2		
STK31	NM_032944				5		
STK32A	NM_145001			4	1		
STK32B	NM_018401				5		
STK32C	NM_173575			3	1		
STK33	NM_030906			2	3		
STK35	NM_080836			1	4		
STK36	NM_015690				5		
STK38L	NM_015000			3	2		
STK39	NM_013233			3	2		
STK4	NM_006282		1	1	3		

Appendix I (*cont'd 15*) **Genes analysed in RNAi screen and the EGFP-EBP50 nuclear localization scores**

Kinase and Phosphatase		No. of shRNA					
		EGFP N-C (shGene/shVC)					
Gene Symbol	Acession No.	≥2.00	1.50-1.99	1.00-1.49	0.51-0.99	0.5-0.11	≤ 0.10
STK40	NM_032017			4			
STK6	NM_003600			4			
STRADA	NM_153335			2	3		
STRADB	NM_018571			3	2		
STYK1	NM_018423			4			
STYX	NM_145251			3	2		
STYXL1	NM_016086			1	4		
SUV39H2	NM_024670				4		
SYK	NM_003177			1	4		
SYT14	NM_153262			2	2		
SYT16	NM_031914			4	1		
SYT17	NM_016524		2	3			
SYT2	NM_177402			3			
SYT4	NM_020783			4	1		
SYT5	NM_003180			5			
SYTL5	NM_138780			2	2		
TAF1	NM_004606			2	3		
TAOK2	NM_004783			3	2		
TA-PP2C	NM_139283			3	2		
TBCK	NM_033115			2	3		
TBK1	NM_013254			2	3		
TEK	NM_000459			5			
TENC1	NM_170754			3	2		
TERF1	NM_003218			5			
TESK1	NM_006285			3	2		
TESK2	NM_007170			5			
TEX14	NM_031272			1	3		
TGFA	NM_003236				3		
TGFB1	NM_000660			1	4		
TGFBR2	NM_001024847			3	2		
THBS1	NM_003246		1	4			
THOC4	NM_005782			3	1		
TIE1	NM_005424			3	2		
TINF2	NM_001099274			3	2		
TJP2	NM_004817			1	4		
TLK1	NM_012290			1	4		
TLK2	NM_001112707			5			
TNF	NM_000594				4		
TNFRSF11A	NM_003839				5		
TNFRSF1B	NM_001066				4		
TNFSF11	NM_033012				5		
TNK1	NM_003985			4	1		
TNK2	NM_005781			2	3		
TNKS	NM_003747			4	1		
TNNI3K	NM_015978			1	4		
TNS1	NM_022648			3	2		
TP53	NM_000546			2	2		
TPTE2	NM_130785			4			

Kinase and Phosphatase		No. of shRNA					
		EGFP N-C (shGene/shVC)					
Gene Symbol	Acession No.	≥2.00	1.50-1.99	1.00-1.49	0.51-0.99	0.5-0.11	≤ 0.10
TRIB2	NM_021643			2	3		
TRIB3	NM_021158				5		
TRIM24	NM_003852			4	1		
TRIM28	NM_005762			3	2		
TRIM33	NM_015906			3	2		
TRIO	NM_007118		1	3			
TRPM6	NM_017662			4	1		
TRPM7	NM_017672			3	1		
TRPV5	NM_019841			4			
TRPV6	NM_018646			1	2		
TRRAP	NM_003496			1	4		
TSC1	NM_000368			4	1		
TSC2	NM_000548			3	2		
TSSK1	NM_032028				4		
TSSK2	NM_053006			1	4		
TSSK3	NM_052841			2	3		
TSSK4	NM_174944			3	1		
TSSK6	NM_032037			1	4		
TTBK2	NM_173500			4	1		
TTK	NM_003318			1	2		
TTN	NM_003319				5		
TTRAP	NM_016614			1	4		
TWF1	NM_002822				4		
TWF2	NM_007284				4		
TXK	NM_003328			2	2		
TYK2	NM_003331			1	4		
TYRO3	NM_006293			2	2		
U2AF1	NM_006758			5			
UBE2D1	NM_003338			2	3		
UBE2D2	NM_003339			2	3		
UBE3A	NM_000462			3	2		
UHMK1	NM_144624				5		
ULK1	NM_003565		1	3	1		
ULK2	NM_014683			4	1		
ULK3	NM_015518				5		
ULK4	NM_017886			1	4		
UNC13B	NM_006377			2	2		
UNK	XM_291786			1	3		
USP39	NM_006590			4	1		
VEGF	NM_003376				5		
VRK1	NM_003384		1		4		
VRK3	NM_016440			4			
WEE1	NM_003390			4	1		
WNK1	NM_018979		1	4			
WNK2	NM_006648			1	4		
WNK4	NM_032387				5		
WT1	NM_024424			4			
WTAP	NM_004906		2	3			

Appendix I (*cont'd 17*) Genes analysed in RNAi screen and the EGFP-EBP50 nuclear localization scores

Kinase and Phosphatase		No. of shRNA					
		EGFP N-C (shGene/shVC)					
Gene Symbol	Acession No.	≥2.00	1.50-1.99	1.00-1.49	0.51-0.99	0.5-0.11	≤ 0.10
XRCC4	NM_003401			3	2		
YES1	NM_005433			2	3		
YSK4	NM_025052	2	1	2			
ZAK	NM_016653			2	3		

   	: Increased nuclear EBP50
   	: Decreased nuclear EBP50

Ubiquitinase and Deubiquitinase		No. of shRNA					
		EGFP N-C (shGene/shVC)					
Gene Symbol	Acession No.	≥2.00	1.50-1.99	1.00-1.49	0.51-0.99	0.5-0.11	≤ 0.10
AKTIP	NM_022476			3	2		
AMFR	NM_001144			2	1		
ANAPC11	NM_016476	1		1	3		
ANKIB1	NM_019004			1	4		
ARIH1	NM_005744			5			
ARIH2	NM_006321			2	2		
ATXN3	NM_001164782			2	3		
ATXN3L	NM_001135995			5			
BAP1	NM_004656	1	2	2			
BARD1	NM_000465			1	4		
BAZ1B	NM_023005			1	4		
BIRC2	NM_001166			3	2		
BIRC3	NM_001165			1	3		
BIRC6	NM_016252			3	2		
BIRC7	NM_022161		3	2			
BIRC8	NM_033341		1	4			
BMI1	NM_005180			2	3		
BRAP	NM_006768	1		3	1		
BRCA1	NM_007294		1	1	1		
BRCC3	NM_024332			3	2		
BTRC	NM_003939			1	4		
C16orf28	NM_023076		2	3			
CBL	NM_005188	1		1	3		
CBLB	NM_170662		1	3			
CBLC	NM_012116		2	1			
CBLL1	NM_024814		3	2			
CBX4	NM_003655		1	4			
CCIN	NM_005893			5			
CCNF	NM_001761			3	2		
CDC34	NM_004359			3	2		
CGRRF1	NM_006568			2	2		
CHFR	NM_018223			2	2		
CNOT4	NM_013316	1		1	3		
COPS5	NM_006837	1	2	2			
COPS6	NM_006833		3	2			
CUL9	NM_015089			3	2		
CYLD	NM_015247	1	1	2	1		
DLK2	NM_023932			1	3		
DTX1	NM_004416	1		3	1		
DTX2	NM_020892			4	1		
DTX3L	NM_138287			1	4		
DTX4	NM_015177			5			
DZIP3	NM_014648		2	3			
EIF3F	NM_003754	3	2				
EIF3FP2	NM_031943	2	2	1			
EIF3H	NM_003756		2	3			
ENC1	NM_003633			5			
FBXL12	NM_017703			2	2		

Appendix I (*cont'd 19*)   Genes analysed in RNAi screen and the EGFP-EBP50 nuclear localization scores

Ubiquitinase and Deubiquitinase		No. of shRNA					
		EGFP N-C (shGene/shVC)					
Gene Symbol	Acession No.	≥2.00	1.50-1.99	1.00-1.49	0.51-0.99	0.5-0.11	≤ 0.10
FBXL13	NM_145032			1	2	1	
FBXL14	NM_152441			4	1		
FBXL15	NM_024326			1	4		
FBXL17	NM_022824			1	4		
FBXL18	NM_024963			5			
FBXL19	NM_019085				5		
FBXL2	NM_012157			4			
FBXL20	NM_032875			1	4		
FBXL22	NM_203373				2	3	
FBXL3	NM_012158		1	4			
FBXL4	NM_012160				4		
FBXL5	NM_012161		1	4			
FBXL6	NM_012162		1	3	1		
FBXL7	NM_012304				4		
FBXL8	NM_018378		1	3	1		
FBXO10	NM_012166			3	2		
FBXO11	NM_012167			3	2		
FBXO15	NM_152676				4		
FBXO16	NM_172366			1	3	1	
FBXO17	NM_024907			3	2		
FBXO18	NM_032807			1	4		
FBXO21	NM_015002			3	2		
FBXO22	NM_012170		1	3			
FBXO24	NM_012172			5			
FBXO25	NM_012173		4	1			
FBXO27	NM_178820		1	3			
FBXO28	NM_015176			2	3		
FBXO3	NM_012175			5			
FBXO30	NM_032145		3	2			
FBXO31	NM_024735				4	1	
FBXO32	NM_058229			4			
FBXO33	NM_203301			2	3		
FBXO34	NM_017943	1		1	2	1	
FBXO36	NM_174899			5			
FBXO39	NM_153230			1	2	2	
FBXO40	NM_016298			1	4		
FBXO41	NM_001080410			1	4		
FBXO42	NM_018994			1	4		
FBXO43	NM_001029860			2	3		
FBXO44	NM_033182				3	1	
FBXO45	NM_001105573			1	4		
FBXO5	NM_012177			4	1		
FBXO6	NM_018438			3	1		
FBXO7	NM_012179			1	4		
FBXO9	NM_012347			3	2		
FBXW11	NM_012300			3	2		
FBXW12	NM_207102			2	3		
FBXW2	NM_012164			3	2		

Ubiquitinase and Deubiquitinase		No. of shRNA					
		EGFP N-C (shGene/shVC)					
Gene Symbol	Acession No.	≥2.00	1.50-1.99	1.00-1.49	0.51-0.99	0.5-0.11	≤ 0.10
FBXW4	NM_022039			1	1		
FBXW5	NM_018998		1	1	1		
FBXW7	NM_018315				4		
FBXW8	NM_012174			4	1		
G2E3	NM_017769		2	3			
GAN	NM_022041			5			
HACE1	NM_020771			5			
HECTD1	NM_015382			2	3		
HECTD2	NM_173497		1	4			
HECTD3	XM_371246			1	4		
HECW1	NM_015052			1	1		
HECW2	XM_038999			1	3		
HERC1	NM_003922			3	2		
HERC2	NM_004667			2	3		
HERC3	NM_014606			4	1		
HERC5	NM_016323			3	2		
HERC6	NM_017912			1	3		
HLTF	NM_003071		1	2	2		
IPP	NM_005897			5			
ITCH	NM_031483			3	1		
IVNS1ABP	NM_006469		1	4			
JOSD1	NM_014876			4	1		
JOSD2	NM_138334			4			
KBTBD10	NM_006063			3	1		
KBTBD11	NM_014867			3	1		
KBTBD3	NM_152433			3	1		
KBTBD4	NM_016506		1	4			
KBTBD5	NM_152393			5			
KBTBD7	NM_032138			5			
KBTBD8	NM_032505			4	1		
KDM2A	NM_012308			1	3		
KDM2B	NM_001005366				5		
KEAP1	NM_012289			4			
KIAA0317	NM_014821			2	2		
KLHL1	NM_020866			4	1		
KLHL10	NM_152467			5			
KLHL11	NM_018143			3	2		
KLHL12	NM_021633	1	2	2			
KLHL2	NM_007246		1	3	1		
KLHL20	NM_014458		2	3			
KLHL21	NM_014851			5			
KLHL22	NM_032775			4	1		
KLHL24	NM_017644			2	3		
KLHL25	NM_022480			5			
KLHL26	NM_018316			5			
KLHL3	NM_017415		1	4	1		
KLHL32	NM_052904			3	2		
KLHL34	NM_153270			2	2		

Ubiquitinase and Deubiquitinase		No. of shRNA					
		EGFP N-C (shGene/shVC)					
Gene Symbol	Acession No.	≥2.00	1.50-1.99	1.00-1.49	0.51-0.99	0.5-0.11	≤ 0.10
KLHL36	NM_024731			4	1		
KLHL4	NM_019117			1	4		
KLHL5	NM_001007075		1	4			
KLHL6	NM_130446		1	4			
KLHL7	NM_018846			4	1		
KLHL8	NM_020803		1	4			
KLHL9	NM_018847			5			
LNX1	NM_032622			1	3	1	
LNX2	NM_153371		1	3			
LONRF1	NM_152271			1	4		
LONRF2	NM_198461		1	2	2		
LONRF3	NM_024778	1		1	3		
LRSAM1	NM_138361	1			4		
LZTR1	NM_006767			4	1		
MAP3K1	XM_042066				5		
MARCH1	NM_017923			3	2		
MARCH2	NM_016496			1	3		
MARCH4	NM_020814				4	1	
MARCH5	NM_017824				3	2	
MARCH5	NM_017824			3	2		
MARCH6	NM_005885			1	4		
MARCH7	NM_022826	1			2		
MARCH9	NM_138396			4	1		
MDM2	NM_002392			5			
MDM4	NM_002393		1		3		
MEX3B	NM_032246				5		
MEX3C	NM_016626			5			
MEX3D	NM_203304			1	3	1	
MGRN1	NM_015246			3	2		
MIB1	NM_020774			2	3		
MIB2	NM_080875		1	4			
MID1	NM_000381		1	2	2		
MID2	NM_012216			1	3		
MKRN1	NM_013446			4	1		
MKRN2	NM_014160		3	2			
MKRN3	NM_005664			2	3		
MKRNP5	NM_030757			2	2		
MLL2	NM_003482			4	1		
MLL3	NM_021230			3	2		
MNAT1	NM_002431			3	2		
MPND	NM_032868			2	3		
MSL2	NM_018133				4	1	
MUL1	NM_024544		3	2			
MYCBP2	NM_015057		3	1			
MYLIP	NM_013262			5			
MYSM1	NM_001085487			2	2	1	
NEDD4	NM_006154			3	2		
NEURL	NM_004210			4	1		

Ubiquitinase and Deubiquitinase		No. of shRNA					
		EGFP N-C (shGene/shVC)					
Gene Symbol	Acession No.	≥2.00	1.50-1.99	1.00-1.49	0.51-0.99	0.5-0.11	≤ 0.10
NFX1	NM_002504			1	4		
NFXL1	NM_152995			3	2		
NHLRC1	NM_198586			3	2		
OTUB1	NM_017670			1	4		
OTUB2	NM_023112	1	1	3			
OTUD3	NM_015207			3	2		
OTUD5	NM_001136157			3	2		
OTUD6A	XM_066765				5		
OTUD6B	NM_016023			1	4		
OTUD7A	NM_130901			3	2		
OTUD7B	NM_020205			2	3		
PAN2	NM_014871		1	3	1		
PARP11	NM_020367			4			
PCGF1	NM_032673				4	1	
PCGF2	NM_007144			3	2		
PCGF3	NM_006315			2	3		
PCGF5	NM_032373			1	4		
PCGF6	NM_032154				5		
PDZRN3	NM_015009				3	2	
PEX10	NM_002617			4	1		
PHF7	NM_016483			2	2		
PHRF1	NM_020901			1	4		
PIAS1	NM_016166		4	1			
PIAS2	NM_004671		1	4			
PIAS3	NM_006099		2	3			
PIAS4	NM_015897			5			
PJA1	NM_022368			1	3		
PJA2	NM_014819			3	2		
PML	NM_002675			1	4		
PRPF19	NM_014502			5			
PRPF8	NM_006445	2	2				
PSMD14	NM_005805		1	4			
PSMD7	NM_002811		1	4			
PXMP3	NM_000318			4	1		
RAD18	NM_020165			4			
RAG1	NM_000448			3	1		
RANBP2	NM_006267	1	3	1			
RAPSN	NM_005055			1	4		
RBBP6	NM_006910			4	1		
RBCK1	NM_006462			3	2		
RBX1	NM_014248			2	3		
RC3H1	NM_172071			3	2		
RC3H2	NM_018835			2	3		
RCHY1	NM_015436			4			
RFFL	NM_057178			4	1		
RFPL1	NM_021026		1	4			
RFPL2	NM_006605			3	2		
RFPL3	NM_006604			1	3		

Appendix I (*cont'd 23*) Genes analysed in RNAi screen and the EGFP-EBP50 nuclear localization scores

Ubiquitinase and Deubiquitinase		No. of shRNA					
		EGFP N-C (shGene/shVC)					
Gene Symbol	Acession No.	≥2.00	1.50-1.99	1.00-1.49	0.51-0.99	0.5-0.11	≤ 0.10
RFPL4A	XM_001718457			3	2		
RFPL4B	NM_001013734			1	4		
RFWD2	NM_001001740			2	2	1	
RING1	NM_002931			1	4		
RLIM	NM_016120			4	1		
RNF10	NM_014868			3	1		
RNF103	NM_005667			3	2		
RNF11	NM_014372			1	3	1	
RNF111	NM_017610	1	2	1	1		
RNF112	NM_007148			2	3		
RNF113A	NM_006978			1	4		
RNF114	NM_018683	1		3	1		
RNF115	NM_014455			4			
RNF121	NM_018320			3	2		
RNF122	NM_024787			2			
RNF123	NM_022064			1	4		
RNF125	NM_017831		2	3			
RNF126	NM_017876			1	3		
RNF128	NM_024539			1	3		
RNF130	NM_018434			4	1		
RNF133	NM_139175			3	2		
RNF138	NM_016271			2	3		
RNF139	NM_007218			4	1		
RNF14	NM_004290			3	2		
RNF141	NM_016422		3	2			
RNF144A	NM_014746			2	3		
RNF144B	NM_182757			4	1		
RNF145	NM_144726		1	3	1		
RNF146	NM_030963			3	2		
RNF149	NM_173647				5		
RNF150	NM_020724			2	3		
RNF152	NM_173557		1	4			
RNF157	XM_290732	1			4		
RNF165	NM_152470			1	3		
RNF166	NM_178841		1	3	1		
RNF167	NM_015528		1	4			
RNF168	NM_152617			5			
RNF169	NM_001098638			5			
RNF17	NM_031277				5		
RNF170	NM_030954				5		
RNF175	NM_173662		3	2			
RNF180	NM_178532				4	1	
RNF181	NM_016494		1		4		
RNF182	NM_152737			5			
RNF185	NM_152267			4			
RNF186	NM_019062			3	2		
RNF187	NM_001010858				5		
RNF19A	NM_015435			2	2		

| Ubiquitinase and Deubiquitinase | | No. of shRNA | | | | | |
| | | EGFP N-C (shGene/shVC) | | | | | |
Gene Symbol	Acession No.	≥2.00	1.50-1.99	1.00-1.49	0.51-0.99	0.5-0.11	≤ 0.10
RNF19B	NM_153341		1	3			
RNF2	NM_007212			2	3		
RNF208	NM_031297			3	2		
RNF213	NM_020914			3	2		
RNF214	NM_207343				4		
RNF220	NM_018150				4	1	
RNF24	NM_007219		1	3	1		
RNF25	NM_022453			1	4		
RNF26	NM_032015		3	1			
RNF31	NM_017999		1	4			
RNF32	NM_030936		1	3			
RNF34	NM_025126		1	4			
RNF39	NM_025236			2	3		
RNF4	NM_002938		1	3	1		
RNF40	NM_014771			3	2		
RNF41	NM_005785			4	1		
RNF43	NM_017763		1	3			
RNF44	NM_014901				2		
RNF5	NM_006913			3	2		
RNF6	NM_005977			2	3		
RNF7	NM_014245			1	4		
RNF8	NM_003958			2	3		
RSPRY1	NM_133368		2	3			
RUFY1	NM_025158				5		
SENP1	NM_014554				5		
SENP2	NM_021627				5		
SENP3	NM_015670				5		
SENP5	NM_152699				5		
SENP6	NM_015571			2	3		
SENP7	NM_020654	1	1	3			
SENP8	NM_145204		2	3			
SH3RF1	NM_020870				4		
SH3RF2	NM_152550				3	1	
SHPRH	NM_173082	1		3	1		
SIAH1	NM_003031			5			
SIAH1L	XM_293360				5		
SIAH2	NM_005067			3	2		
SKP2	NM_005983		1	4			
SMURF1	NM_020429			1	3		
SMURF2	NM_022739			2	2		
STAMBP	NM_006463	1		4			
STAMBPL1	NM_020799		3	1	1		
STUB1	NM_005861	1	2	2			
TAF1D	NM_024116			2	3		
TCEB3	NM_003198	1		1	3		
TDRD4	NM_019038				5		
TMEM189-UBE2V1	NM_003349		1	3			
TNFAIP3	NM_006290		1	4			

Appendix I (*cont'd 25*) Genes analysed in RNAi screen and the EGFP-EBP50 nuclear localization scores

Ubiquitinase and Deubiquitinase		No. of shRNA					
		EGFP N-C (shGene/shVC)					
Gene Symbol	Acession No.	≥2.00	1.50-1.99	1.00-1.49	0.51-0.99	0.5-0.11	≤ 0.10
TOPORS	NM_005802			5			
TRAF2	NM_021138			2	2		
TRAF3	NM_003300			5			
TRAF4	NM_004295			3	2		
TRAF5	NM_004619			3	2		
TRAF6	NM_004620			3	2		
TRAF7	NM_032271			1	4		
TRAIP	NM_005879			3	2		
TRIM10	NM_006778				4		
TRIM11	NM_145214			5			
TRIM13	NM_005798			5			
TRIM15	NM_033229		1	3			
TRIM2	NM_015271			1	4		
TRIM21	NM_003141				5		
TRIM22	NM_006074			2	1		
TRIM23	NM_001656			3	2		
TRIM24	NM_003852			2	3		
TRIM25	NM_005082			3	2		
TRIM26	NM_003449		1	4			
TRIM27	NM_006510			5			
TRIM28	NM_005762			1	4		
TRIM3	NM_006458			4	1		
TRIM31	NM_007028			4	1		
TRIM32	NM_012210			1	4		
TRIM33	NM_015906		1	3	1		
TRIM34	NM_021616			3	1		
TRIM35	NM_015066			3	1		
TRIM36	NM_018700				5		
TRIM37	NM_015294			5			
TRIM38	NM_006355			5			
TRIM39	NM_021253			1	3		
TRIM4	NM_033017			2	3		
TRIM40	NM_138700			2	2		
TRIM41	NM_033549			5			
TRIM43	NM_138800		2	3			
TRIM45	NM_025188			1	4		
TRIM46	NM_025058		2	3			
TRIM47	NM_033452			3	2		
TRIM48	NM_024114		4	1			
TRIM49	NM_020358		1	4			
TRIM5	NM_033034		1	2			
TRIM50	NM_178125		2	3			
TRIM52	NM_032765		4	1			
TRIM54	NM_032546			5			
TRIM56	NM_030961				5		
TRIM59	NM_173084			5			
TRIM6	NM_058166			2	3		
TRIM60	NM_152620			5			

Ubiquitinase and Deubiquitinase		No. of shRNA					
		EGFP N-C (shGene/shVC)					
Gene Symbol	Acession No.	≥2.00	1.50-1.99	1.00-1.49	0.51-0.99	0.5-0.11	≤ 0.10
TRIM63	NM_032588			1	4		
TRIM65	NM_173547				4	1	
TRIM67	NM_001004342			1	3		
TRIM68	NM_018073			3	2		
TRIM69	NM_080745	1		1	3		
TRIM7	NM_033342			5			
TRIM72	NM_001008274				4	1	
TRIM73	NM_198924			2	3		
TRIM74	NM_198853			4	1		
TRIM8	NM_030912			5			
TRIM9	NM_015163		1	4			
TRIML1	NM_178556			5			
TRIP12	NM_004238		1	3	1		
TSG101	NM_006292		1	4			
TTC3	NM_003316			1	3		
UBE2A	NM_003336			3	1		
UBE2B	NM_003337			2	3		
UBE2C	NM_007019		1	3			
UBE2D1	NM_003338			4	1		
UBE2D2	NM_003339			4	1		
UBE2D3	NM_003340			3	2		
UBE2D4	NM_015983		1	4			
UBE2E1	NM_003341			4	1		
UBE2E2	NM_152653	1			2		
UBE2E3	NM_006357		2	3			
UBE2F	NM_080678			5			
UBE2G1	NM_003342	1		1	3		
UBE2G2	NM_003343		1	3	1		
UBE2H	NM_003344			3	2		
UBE2I	NM_003345	1	2	2			
UBE2J1	NM_016021		1	4			
UBE2J2	NM_058167			5			
UBE2K	NM_005339			1	4		
UBE2L3	NM_003347			2	3		
UBE2L6	NM_004223			2	1		
UBE2M	NM_003969			1	4		
UBE2N	NM_003348			5			
UBE2O	NM_022066			4	1		
UBE2Q1	NM_017582	1		4			
UBE2Q2	NM_173469		3	2			
UBE2R2	NM_017811			4	1		
UBE2S	NM_014501			2	3		
UBE2T	NM_014176		3	2			
UBE2U	NM_152489			4	1		
UBE2V1	NM_021988			1	4		
UBE2V2	NM_003350			1	4		
UBE2W	NM_018299			1	4		
UBE2Z	NM_023079			2			

Appendix I (*cont'd 27*)   Genes analysed in RNAi screen and the EGFP-EBP50 nuclear localization scores

Ubiquitinase and Deubiquitinase		No. of shRNA					
		EGFP N-C (shGene/shVC)					
Gene Symbol	Acession No.	≥2.00	1.50-1.99	1.00-1.49	0.51-0.99	0.5-0.11	≤ 0.10
UBE3A	NM_000462			5			
UBE3B	NM_130466			4	1		
UBE3C	NM_014671		1	3			
UBE4A	NM_004788			1	4		
UBE4B	NM_006048	1		4			
UBOX5	NM_014948			2	3		
UBR1	NM_174916		1	4			
UBR3	NM_172070			5			
UBR5	NM_015902			1	4		
UCHL1	NM_004181			1	4		
UCHL3	NM_006002		4	1			
UCHL5	NM_015984			4	1		
UEVLD	NM_018314			3	1		
UFD1L	NM_005659			3	2		
UHRF1	NM_013282			3	2		
UHRF2	NM_152306			1	3		
USP1	NM_003368			3	2		
USP10	NM_005153			5			
USP11	NM_004651			2	3		
USP12	NM_182488		2	3			
USP13	NM_003940			3	2		
USP14	NM_005151	1	2	2			
USP15	NM_006313		1	4			
USP16	NM_006447		1	3	1		
USP17L2	NM_201402		1	3	1		
USP17L6P	NM_212553			2	3		
USP18	NM_017414				5		
USP19	XM_496642			3	2		
USP2	NM_004205		1	3	1		
USP20	NM_006676	1	1	3			
USP21	NM_012475			3	2		
USP22	NM_015276				5		
USP24	NM_015306				5		
USP25	NM_013396			3	2		
USP26	NM_031907		2	3			
USP28	NM_020886				5		
USP29	NM_020903			1	4		
USP3	NM_006537				3	2	
USP30	NM_032663			4	1		
USP31	NM_020718			3	2		
USP32	NM_032582			5			
USP33	NM_015017			4	1		
USP34	NM_014709	2		2	1		
USP35	NM_020798				5		
USP36	NM_025090		2	2	1		
USP37	NM_020935		1	2	2		
USP38	NM_032557		1	2	2		
USP39	NM_006590			3	2		

Appendix I (*cont'd 28*) Genes analysed in RNAi screen and the EGFP-EBP50 nuclear localization scores

Ubiquitinase and Deubiquitinase		No. of shRNA					
		EGFP N-C (shGene/shVC)					
Gene Symbol	Acession No.	≥2.00	1.50-1.99	1.00-1.49	0.51-0.99	0.5-0.11	≤ 0.10
USP4	NM_003363			3	2		
USP40	NM_018218		1	3	1		
USP42	NM_032172			1	4		
USP43	NM_153210				4	1	
USP44	NM_032147			5			
USP45	NM_001080481				4	1	
USP46	NM_022832		1	4			
USP47	NM_017944		1	4			
USP48	NM_032236			4	1		
USP49	NM_018561			1	4		
USP5	NM_003481			2	3		
USP50	NM_203494			3	2		
USP51	NM_201286		1	2	2		
USP53	XM_052597		1	1	2		
USP54	NM_152586		1	2	2		
USP6	NM_004505			3	2		
USP7	NM_003470			3	2		
USP8	NM_005154				5		
USP9X	NM_004652			4			
USP9Y	NM_004652	1	1	2			
USPL1	NM_005800			4	1		
VCPIP1	NM_025054	1		2	2		
VPS11	NM_021729				5		
VPS41	NM_014396			3	2		
VPS8	NM_015303			1	4		
WWP1	NM_007013			3	2		
WWP2	NM_007014			5			
XIAP	NM_001167		1	1	2		
YOD1	NM_018566			1	3		
ZNF598	NM_178167			1	3		
ZNF645	NM_152577			5			
ZNRF1	NM_032268	1			3	1	
ZNRF2	NM_147128			3	2		
ZNRF3	NM_032173		1	4			
ZNRF4	NM_181710		1	4			
ZRANB1	NM_017580			2	3		
ZSWIM2	NM_182521		1	3	1		

Appendix I (*cont'd 29*) Genes analysed in RNAi screen and the EGFP-EBP50 nuclear localization scores

Palmitoyltransferase		No. of shRNA					
		EGFP N-C (shGene/shVC)					
Gene Symbol	Acession No.	≥2.00	1.50-1.99	1.00-1.49	0.51-0.99	0.5-0.11	≤ 0.10
ZDHHC1	NM_013304			2	3		
ZDHHC2	NM_016353			4	1		
ZDHHC3	NM_016598			3	1		
ZDHHC4	NM_018106			4	1		
ZDHHC6	NM_022494			3	1		
ZDHHC7	NM_017740			3	1		
ZDHHC9	NM_016032			2	3		
ZDHHC11	NM_024786			1	4		
ZDHHC13	NM_019028			0	4		
ZDHHC14	NM_024630			3	1		
ZDHHC15	NM_144969			3	1		
ZDHHC16	NM_032327			3	1		
ZDHHC17	NM_015336			3	1		
ZDHHC18	NM_032283			2	2		
ZDHHC19	NM_144637			3	2		
ZDHHC20	NM_153251			3	1		
ZDHHC21	NM_178566			4	1		
ZDHHC22	NM_174976			3	1		
ZDHHC23	NM_173570			5	0		